



Fall 2003

Delineation of Landslide Slip Surfaces Using Ground Penetrating Radar as Compared and Contrasted with Existing Slip Surface Data: Evaluation of GPR for Landslide Slip Surface Determination

Michael E. (Michael Eric) Hutchinson
Western Washington University, mhutchinson@geoengineers.com

Follow this and additional works at: <https://cedar.wwu.edu/wwuet>



Part of the [Geology Commons](#)

Recommended Citation

Hutchinson, Michael E. (Michael Eric), "Delineation of Landslide Slip Surfaces Using Ground Penetrating Radar as Compared and Contrasted with Existing Slip Surface Data: Evaluation of GPR for Landslide Slip Surface Determination" (2003). *WWU Graduate School Collection*. 665.
<https://cedar.wwu.edu/wwuet/665>

This Masters Thesis is brought to you for free and open access by the WWU Graduate and Undergraduate Scholarship at Western CEDAR. It has been accepted for inclusion in WWU Graduate School Collection by an authorized administrator of Western CEDAR. For more information, please contact westerncedar@wwu.edu.

Delineation of Landslide Slip Surfaces Using Ground Penetrating Radar as Compared and
Contrasted with Existing Slip Surface Data: Evaluation of GPR for Landslide Slip
Surface Determination

by

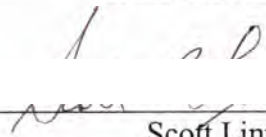
Michael E. Hutchinson, L.G., L.Hg.

Accepted in Partial Completion
of the Requirements for the Degree
Master of Science

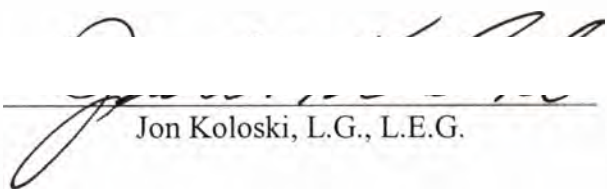
Moheb A. Ghali, Dean of Graduate School

ADVISORY COMMITTEE

Chair, Bernard Housen, L.G.




Scott Linneman, L.G.



Jon Koloski, L.G., L.E.G.

MASTER'S THESIS

In presenting this thesis in partial fulfillment of the requirements for a master's degree at Western Washington University, I agree that the Library shall make its copies freely available for inspection. I further agree that copying of this thesis project in whole or in part is allowable only for scholarly purposes. It is understood, however, that any copying or publication of this thesis for commercial purposes, or for financial gain, shall not be allowed without my written permission.

Signature  _____

Date

11/30/03 _____

MASTER'S THESIS

In presenting this thesis in partial fulfillment of the requirements for a master's degree at Western Washington University, I grant to Western Washington University the non-exclusive royalty-free right to archive, reproduce, distribute, and display the thesis in any and all forms, including electronic format, via any digital library mechanisms maintained by WWU.

I represent and warrant this is my original work, and does not infringe or violate any rights of others. I warrant that I have obtained written permissions from the owner of any third party copyrighted material included in these files.

I acknowledge that I retain ownership rights to the copyright of this work, including but not limited to the right to use all or part of this work in future works, such as articles or books.

Library users are granted permission for individual, research and non-commercial reproduction of this work for educational purposes only. Any further digital posting of this document requires specific permission from the author.

Any copying or publication of this thesis for commercial purposes, or for financial gain, is not allowed without my written permission.

Michael Hutchinson
February 22, 2018

Delineation of Landslide Slip Surfaces Using Ground Penetrating Radar as Compared and
Contrasted with Existing Slip Surface Data: Evaluation of GPR for Landslide Slip
Surface Determination

A Thesis
Presented to the Faculty of
Western Washington University

In Partial Completion
of the Requirements for the Degree
Master of Science

by
Michael E. Hutchinson, L.G., L.Hg.
December 2003

ABSTRACT

Ground penetrating radar (GPR) was used to investigate two landslides within the South Puget Sound region to evaluate if this technology could be used to delineate slip surface location. The internal structures of two landslides with similar stratigraphic and geographic settings in the South Puget Sound Region were evaluated using GPR. For the two landslides studied, results of prior geologic and geotechnical work identified the location and extent of each landslide slip surface. Longitudinal and latitudinal GPR transects were completed on each landslide mass to map subsurface radar reflection amplitudes (radargrams) and times. To convert radar travel times to depths, radar velocities were determined using common midpoint surveys. GPR data were compared to previously collected geotechnical data characterizing the landslide mass using known techniques. Results show a correlation between landslide slip surface location and high amplitude reflectors displayed on radargrams on a landslide mass consisting predominantly of sands and gravels providing optimum radar penetration. The GPR technique was not successful on the landslide mass with higher silt content, which resulted in a larger degree of radar wave attenuation.

TABLE OF CONTENTS

ABSTRACT.....	iv
LIST OF TABLES AND FIGURES.....	vi
INTRODUCTION.....	1
GENERAL	1
GROUND PENETRATING RADAR	2
STUDY AREA	6
Eldon Landslide	8
Tahuya Landslide	9
METHODOLOGY.....	10
INVESTIGATION.....	12
ELDON LANDSLIDE.....	13
Eldon Transect Results	13
Eldon Transect Discussion	16
TAHUYA LANDSLIDE.....	17
Tahuya Transect Results	17
Tahuya Transect Discussion	19
DISCUSSION AND CONCLUSIONS.....	20
REFERENCES.....	24

LIST OF TABLES AND FIGURES

Table 1 Typical Dielectric Constant, Electrical Conductivity and Velocity Observed in Common Geological Materials	26
Table 2 Common Midpoint Results	27
Figure 1 Simplified Diagram Showing Components of GPR System	28
Figure 2 Typical Radargram Displayed as a Linscan and Oscilloscope Trace	29
Figure 3 Location of Eldon and Tahuya Landslides in Washington State	30
Figure 4 Location of Eldon Landslide	31
Figure 5 Eldon Landslide Features	32
Figure 6 Eldon Landslide Cross Section	33
Figure 7 Location of Tahuya Landslide	34
Figure 8 Tahuya Landslide Features	35
Figure 9 Tahuya Landslide Cross Section	36
Figure 10 Simplified CMP Diagram	37
Figure 11 Eldon Landslide CMP Survey	38
Figure 12 Eldon Landslide Transect A	39
Figure 13 Eldon Landslide Transect B	40
Figure 14 Eldon Landslide Transect C	41
Figure 15 Eldon Landslide Transect D	42
Figure 16 Eldon Landslide Transect E	43
Figure 17 Eldon Landslide Transect F	44
Figure 18 Eldon Landslide Transect G	45
Figure 19 Eldon Landslide Transect H	46
Figure 20 Eldon Landslide Transect N Winter Surveys	47
Figure 21 Seasonal Comparisons Transects N and A	48
Figure 22 Eldon Landslide Transect O Winter Survey	49
Figure 23 Seasonal Comparisons Transects O and E	50
Figure 24 Tahuya Landslide CMP Survey	51
Figure 25 Tahuya Landslide Transect I	52
Figure 26 Tahuya Landslide Transect J	53
Figure 27 Tahuya Landslide Transect K	54
Figure 28 Tahuya Landslide Transect L	55
Figure 29 Tahuya Landslide Transect M	56

INTRODUCTION

GENERAL

In the United States annual economic losses due to landslides have been estimated to range from \$1 billion to \$2 billion (Schuster, 1996). With continued housing development in landslide-prone areas, landslide occurrence and monetary losses will persist and most likely increase. Expedient evaluation and stabilization of landslides helps to reduce their economic impact and can improve safety to life as well. Landslide slip surface delineation is critical for proper mitigation design measures (Holtz and Hubatka, 1996).

The slip surfaces of landslides are commonly characterized through the use of subsurface exploration such as borings, test pits, etc., together with instrumentation such as tiltmeters, inclinometers, extensometers and/or piezometers which offer discrete data at specific locations. Borings and instrumentation for landslide monitoring and mitigation are often sparse because of the high cost of these proven methods. The slip surface must then be determined by interpretation of the data and extrapolation between measured locations. Despite some advances in technology (e.g. inclinometers) further development of new instrumentation technology for monitoring landslides and delineating slip surfaces has been limited. The slow-paced gains in landslide monitoring have been attributed to the following (Mikkelson, 1996):

- Geotechnical industry is small and highly specialized
- Support for research and development has dwindled

With new technologies developing slowly to characterize slip surfaces, and with more development in landslide prone areas, there is a clear need for new techniques to facilitate slip surface characterization. This project addresses one such technique that could potentially generate three-dimensional constraints of landslide slip surfaces through visual and numerical methods: ground penetrating radar (GPR).

GROUND PENETRATING RADAR

Ground penetrating radar (Figure 1) involves the transmission of high frequency electromagnetic radio (radar) pulses into the earth and measuring the time elapsed between transmission of the waves into the subsurface, reflection of a portion of the incident waves off of a sub-surface discontinuity, and reception back at a surface antenna (Conyers and Goodman, 1997). Reflected waves produce a radargram from single oscilloscope traces (Figure 2). This relatively new technology, pioneered by Ulrickson (1982), enables high-resolution mapping of bedrock and soil stratigraphy (Davis and Annan, 1989). Typical GPR frequencies range from 15-1000 Mhz with corresponding wavelengths of ~2 m to ~0.1 m. Portions of the wave are reflected at discontinuities in the underground back to the surface and recorded (Grasmuck and Green, 1996). Subsurface properties that produce reflections occur at the interfaces varying electrical and magnetic properties. To characterize these reflections the relative dielectric constant of the subsurface materials must be known. The dielectric constant can be thought of as a measure of the ability of a material within an electromagnetic field to respond to propagated electromagnetic waves (Olhoeft, 1981). A larger amplitude reflection will be produced where there is a greater difference between the dielectric constants at an

interface (Conyers and Goodman, 1997). The magnitude of the reflection generated at an interface can be quantified using equation (1) below if the dielectric constant is known (Sellman et al., 1983; Walden and Hosken, 1985; Davis and Annan, 1989):

$$R = [(K_1)^{1/2} - (K_2)^{1/2}] / [(K_1)^{1/2} + (K_2)^{1/2}] \quad (1)$$

R = reflection coefficient

K_1 = dielectric constant of overlying material

K_2 = dielectric constant of underlying material

In order to generate a significant reflection, the change in dielectric constants between two materials must occur across an interval of time appropriate for the radar frequency being used. The degree to which the radar reflections can be detected is a function of the original signal strength and the amplitude of the reflected waves. The higher the amplitude, the more easily detectable the reflections become. Lower amplitude reflections usually occur when there are only small differences in the dielectric constants between layers (Conyers and Goodman, 1997). The arrival times and amplitudes of reflected signals provide the information necessary to construct a subsurface image and can be used to constrain the differences in subsurface physical properties that are responsible for the reflection. These differences can be represented numerically, by the reflection coefficients and visually, by the profiles.

Electrical properties of geological materials are primarily controlled by the water content (Topp et al., 1980). Variations in the electrical properties of soils are usually associated with volumetric water content, which, in turn, give rise to radar reflections. In previous studies by Davis and Annan (1989), fresh water has been determined to have a

dielectric constant (unitless value) of approximately 80, saturated sand approximately 20-30 and dry sand approximately 3-5 (Table 1) (Davis and Annan, 1989). Based on these studies by Topp et al (1980), Davis and Annan (1989) and equation 1, a saturated/dry interface will provide a prominent reflection.

Over the past 10 years, GPR studies in a wide variety of geomorphic and geologic settings have revealed detailed stratigraphic information as well as information regarding GPR uses and limitations. GPR studies have predominantly focused on the application of GPR and not the theory of its operation. Davis and Annan (1989) describe GPR concepts, electrical properties, radar system characteristics, equipment, methods and interpretation in detail. Davis and Annan explain the relationship between the resolvable thicknesses of a reflector as related to subsurface velocity at varying antennae velocities and the thickness of a reflector. Future studies should provide further information regarding the theory of GPR operation.

Applicable studies involving the application of GPR and its uses and limitations in various geologic settings have been conducted. Jol (1995) demonstrated that the vertical resolution of GPR increases with increasing radar frequency and that the depth of penetration increases with decreasing radar frequency. Jol also concluded that the resolvable thickness of a reflector is a function of the wavelength of the antennae and the subsurface radar velocity. With decreasing antennae frequencies and material velocities the overall thickness of the reflector would need to be increased to provide a reflection. Jol determined a 200 MHz antennae was able to resolve a reflector of an approximate thickness of 0.25 m with a subsurface velocity of 0.20 m/ns. Jol (1995) also

demonstrated that there is a correlation between increasing antennae frequencies and depth penetration. Jol utilized a 25, 50, 100 and 200 MHz antennae in deltaic sediments and visually interpreted radargrams showing that with increasing antennae frequencies the return signal from a reflector increased but the overall depth penetration decreased while the overall resolution increased.

Hruska and Hubatka (2000) describe the application of GPR to investigate landslide slip surfaces in the Czech Republic, but their study lacked the detail for development of a methodology for future investigations. Hruska and Hubatka determined that geophysical methods provide information about the internal structure (cracks and fissures) of landslides providing possible mitigation solutions.

Barnhardt and Kayen (2000) used GPR to investigate the internal structure of two landslides in Anchorage, Alaska, that resulted from the 1964 earthquake. GPR data was compared with previous investigations and it was determined that GPR reflection surveys accurately reproduced subsurface geometry of horst and graben structures and imaged finer scale images such as ground cracks and fissures. A pulseEKKO 100 GPR system was used to collect 1000 meters of reflection profiles on two separate landslide masses during this study. The stratigraphy of the subsurface materials in this study area consisted of 1) glacial till unconformably overlying bedrock; 2) silty clay of the Bootlegger Cove Formation resting on till or bedrock, and; 3) outwash sand and gravel on the surface (Barnhardt and Kayen, 2000). This study was limited by the propagation of radar waves into the subsurface and only provided information regarding the internal structure of the

landslide mass (horst and graben features) with no insight into landslide slip surface location.

Bruno and Marlillier (2000) tested GPR using a 100 MHz antenna (no other system information was provided) on a landslide in the Swiss Alps to help reveal geologic structures and processes and thus help devise mitigation strategies. The geology in this study area consisted of Jurassic shale and gypsum. This study found that GPR profiling provided limited success due to the GPR signals being very “short” due to the high conductivity of the subsurface and this technique is expected to be site dependent if to be successfully applied to landslide evaluation. Bruno and Marlillier provided no further information and the GPR section (not provided) was deemed unsatisfactory for review.

Knight (2001) determined through review of numerous journal articles that GPR offers a non-invasive geophysical technique to estimate hydrogeologic properties such as water content, porosity, and permeability. Knight also determined that GPR can provide useful information about large scale structures within the top few tens of meters of earth but is limited in the ability to obtain accurate, quantitative information about subsurface properties of interest at the required scale due to the spatial complexity of the subsurface. Knight’s review does not expand on the limits of GPR and what is defined as “accurate, quantitative information.”

STUDY AREA

The Puget Sound Lowland is a north-south trending structural depression bordered on the west by the Olympic Mountains and the east by the Cascade Mountains

(Figure 3). Repeated glaciations during the Pleistocene have carved the Puget Lowlands leaving thick deposits of glacial tills, glacio-lacustrine silts and clays, and glacio-fluvial sands and gravels. These glacial deposits are underlain by Tertiary bedrock units primarily associated with the Crescent terrane, a complex sequence of marine basalts and terrestrial and marine sedimentary rocks (Babcock, et al., 1994). Hillslopes in the area are commonly oversteepened by erosion or landslides and have been deeply incised by streams. Regional susceptibility to landslides mainly reflects low-strength, thin soils underlain by relatively impermeable high-strength glacial sediments and/or bedrock. The Puget Lowland is also characterized by abundant rain or combination of rain and snow.

Many landslide types occur in the Puget Lowland including falls and topples, slides, spreads and flows. The purpose of this research is to evaluate GPR reflection amplitudes for delineating slip surfaces of landslides in the Puget Lowland. The objective of this project is to attempt to characterize known slip surfaces of landslides typical within the Puget Lowland and determine the applicability of GPR. GPR may provide discrete information regarding reflection amplitudes at the slip surfaces of landslides and contribute to future research in the area of GPR and the delineation of slip surfaces using this method.

To support this study drilling logs and inclinometer data for many landslides within the Puget Sound Lowland were reviewed. Resources for the data included GeoEngineers Inc., Washington State Department of Transportation and Mason County Department of Public Works. Landslides with well-determined slip surfaces were selected from the existing data and reports and are discussed further below.

Eldon Landslide

The Eldon Landslide (Figure 4) is in the southern portion of the Puget Lowland located approximately 23 miles north of Shelton along State Route 101. The Eldon landslide is approximately 300 meters long and is 73 meters wide near the headscarp and 128 meters wide near the toe (Figure 5). The project area consists of four distinct engineering geologic units. These units (from stratigraphically lowest to highest) are: Unit 4, Bedrock, consisting of fine grained basalt; Unit 3, Glacial Till, consisting of very dense, dark brown to gray, silty sandy gravel with cobbles and boulders; Unit 2, Glacio-lacustrine Silts and Clays consisting of stiff to very hard, dark gray, clayey silt to silty clay; Unit 1, Glacial Outwash Sands and Gravels, consisting of loose to very dense, brown to gray, sandy gravels and silty sands (Figure 6) (WSDOT, 2000).

The Eldon Landslide was chosen for this study based on the detailed data interpreting the landslide slip surface. During late winter 1980 a series of four test borings were advanced within the landslide. Due to lack of project information in the files, it is not clear what types of instrumentation were installed to monitor the landslide at this time, although at least one of the borings had an inclinometer installed. In February 1995, after renewed landslide activity, a series of new test borings were advanced into the landslide. A total of six test borings at three locations were advanced to determine subsurface conditions, obtain disturbed and undisturbed samples and to install slope inclinometers and open standpipe piezometers to monitor ground movement and groundwater, respectively. During the winter of 1998-1999 abnormally high

precipitation resulted in movement of the Eldon Landslide and catastrophic failures of another two very large landslides adjacent to the site (WSDOT, 2000).

WSDOT found that movement within the landslide appears to be translational in nature (sliding block). Based on monitoring of the slope inclinometers and recent measurements of both the sheared slope inclinometers and piezometers the depth of the failure surface ranges from 6 to 15 meters below ground surface (WSDOT, 2000).

The Eldon landslide took over 5 years to be characterized while nearby catastrophic failures occurred indicating the need for expeditious characterizations of landslide slip surfaces.

Tahuya Landslide

The Tahuya Landslide is in the southern portion of the Puget Lowland located approximately 1 mile southeast of Tahuya, Washington (Figure 7). The Tahuya landslide is approximately 110 meters long and is 150 meters wide near the headscarp and 340 meters wide near the toe (Figure 8). The soils consist of glacial outwash that are either in situ or have been reworked as the result of slope processes and landslide activities (Figure 9).

The Tahuya Landslide was chosen for this study based on the detailed data available delineating the landslide slip surface. The landslide is a complex rotational slide with several smaller landslides that have coalesced to form a large feature. The Tahuya landslide contrasts the Eldon landslide due to the higher silt content located in the upper few meters and that it is a rotational feature compared to a translational feature.

Previous investigations (GeoEngineers, 1998) determine the undisturbed outwash deposits located in the upper slope consist of loose sand with varying quantities of silt and gravel in the upper 6 meters grading downward to very dense sand, gravel and very hard silt. The mid-slope soils consist of landslide deposits to a depth of approximately 7 meters. The landslide deposits consist of loose, reworked sand, gravel and silt outwash deposits. The landslide deposits rest on a hard, intact silt layer, which in turn overlies undisturbed outwash deposits consisting of interbedded very dense silty gravel, clean to silty sand and occasional silt beds. The thickness of individual beds is approximately 1 to 5 meters. The soil along the lower portion of the slope consists of loose to medium dense soil near the surface, overlying very dense interbedded sand and gravel (GeoEngineers, 1998).

METHODOLOGY

In an attempt to develop an expeditious delineation method for slip surface location, GPR transects were completed on the 2 displaced landslide masses. Transect locations were chosen where previously completed roads and/or trails were located. These transects were extended across the displaced landslide mass, flanks, crown, and/or toe of the landslides. GPR profiles were then compared against existing monitoring data for reflections that exist at depths of known slip surfaces. Two transects for a single slide were repeated during the winter months of 2002 to compare seasonal variations of the reflected radar signals.

The Eldon and Tahuya landslides were surveyed with a Geophysical Survey Systems, Inc. (GSSI) SIR-2000 GPR system. The system includes a transmitter, receiver,

respective cables and a control unit. A shielded 200MHz and unshielded 50 MHz transmitter/receiver (antennae) were used. The transmitter sends a short pulse of electromagnetic energy into the ground. The signal reflects off interfaces having contrasting dielectric constants and returns to the receiver. The receiver measures the two-way travel time of the signal in nanoseconds (ns). The return signals were post-processed using RADAN-NT software (GSSI), and converted into images (radargrams) that depict the reflections of radar waves in the subsurface.

Post-processing of 200 MHz transects for the Eldon landslide were performed using a horizontal high-pass filter to remove visible bands of ringing. Ringing is displayed as horizontal banding that appears in many GPR records. These bands can obscure reflection data that would otherwise be visible (Conyers and Goodman, 1997). Post-processing of 200 Mhz transect for the Tahuya transects was performed using a range gain of 10 decibels to compensate for reduction in reflection amplitude. Topography was surveyed using a total station and elevations were corrected during radargram transect post processing.

A 50 MHz common midpoint (CMP) survey was performed on the Eldon and Tahuya landslides to determine velocity of radar through the ground and determine an appropriate scale for the completed transects. During a CMP survey, a reflection is produced where a reflector is centered on a single point (Figure 10). The transmitter and reflector are moved in opposite directions at equal intervals. By separating the transmitter and receiver about a single point, the system will measure the travel time along multiple paths with the travel times varying in a hyperbolic manner. By graphing the distance (x^2)

versus return time (t^2) the slope of the plotted reflector will give the velocity (v^2). This allows the conversion from travel time to depth (Figure 10). Dielectric constants, electrical conductivities and velocity observed in common geologic materials were determined by Davis and Annan (1989) (Table 1).

The electric permittivity controls radar wave velocity, while the electrical conductivity has a large effect on attenuation of radar waves (Knight, 2001). High silt-content soils will effectively have a higher electrical conductivity, lower velocity, and greater attenuation (Davis and Annan, 1979). Limited radar signal loss based on electrical conductivity, velocity, and attenuation are considered “low loss conditions” (low attenuation). “Low loss conditions” are expressed mathematically by the inequality $\sigma/\omega\epsilon < 1$ where σ is electrical conductivity, ω is angular frequency and ϵ is dielectric permittivity. This equation indicates that GPR cannot be used where conductivity is too high; high values of σ result in highly attenuated medium. Clay mineral content (high σ) on the order of 5-10% can reduce the penetration depth of radar to less than a meter (Knight, 2001).

GPR transect profiles were reviewed and amplitude reflectors were noted and marked and compared against existing boring data to evaluate correlation of GPR data with confirmed conventional methods currently used for slip surface.

INVESTIGATION

ELDON LANDSLIDE

Eight GPR transects (A through H) using a 200 MHz antenna were completed on September 07, 2002, on various areas of the landslide (Figure 5). A common midpoint

survey (CMP) was completed on October 25, 2002, using a 50 MHz antenna along transect E (Figure 5). Two transects were repeated on February 15, 2003, to compare seasonal variations of radar signals. The transects for this portion of the study were transects A and E as completed on September 07, 2002.

Eldon Transect Results

CMP Survey

A hyperbolic reflection was seen at approximately 90 ns at 3.24 m of separation extending to 140 ns at 14.31 m of separation (Figure 11). Calculation of subsurface velocity using CMP surveys was completed as described. The CMP results indicate the average velocity of subsurface material to be 0.129 m/ns. This would equate to a depth scale of 12.9 m per 100 ns (Table 2). This average velocity was used for all subsurface units and specific velocities for each unit were not determined.

Transect A

A 120 meter transect was completed approximately 85 meters upslope from the toe of the landslide mass. Transect A was the longest and crossed the east flank of the slide (Figure 5). Surface material consisted of a mixture of coarse sand and gravel. The radargram display for this transect indicates a prominent reflector at approximately 6 to 8 meters below ground surface (bgs) (Figure 12). Where transect A crosses the south flank of the landslide this prominent reflection loses strength.

Transect B

A 30 meter transect was completed approximately 85 to 115 meters upslope from the toe of the landslide mass (Figure 5). Surface material consisted of a mixture of forest

duff and coarse sand and gravel. The radargram display for this transect indicates a prominent reflector at approximately 6 to 8 meters bgs (Figure 13).

Transect C

A 45 meter transect was completed approximately 85 to 130 meters upslope from the toe of the landslide mass (Figure 5). Surface material consisted of a mixture of forest duff. The radargram display for this transect indicates a prominent reflector at approximately 6 to 8 meters bgs (Figure 14).

Transect D

A 25 meter transect was completed approximately 125 meters upslope from the toe of the landslide mass (Figure 5). Surface material consisted of a mixture of forest duff. The radargram display for this transect indicates a prominent reflector at approximately 6 to 8 meters bgs (Figure 15).

Transect E

A 70 meter transect was completed approximately 140 meters upslope from the toe of the landslide mass (Figure 5). Surface material consisted of a mixture of forest duff. The radargram display for this transect indicates a prominent reflector at approximately 6 to 8 meters bgs. Where transect E crosses the west flank this prominent reflection loses strength (Figure 16).

Transect F

A 30 meter transect was completed approximately 140 to 170 meters upslope from the toe of the landslide mass (Figure 5). Surface material consisted of a mixture of forest duff and coarse sand and gravel. The radargram display for this transect indicates a

reflector at approximately 6 to 8 meters bgs. A reflector can also be seen at the location where a previously installed piezometer is located (Figure 17).

Transect G

A 30 meter transect was completed approximately 250 meters upslope from the toe of the landslide mass (Figure 5). Surface material consisted of a mixture of forest duff and coarse sand and gravel. The radargram display for this transect indicates a reflector at approximately 6 to 8 meters bgs. A reflector can also be seen at the location where a previously installed piezometer is located (Figure 18).

Transect H

A 15 meter was completed approximately 230 to 250 meters upslope from the toe of the landslide mass (Figure 5). Surface material consisted of a mixture of forest duff and coarse sand and gravel. The radargram display for this transect indicates a prominent reflector at approximately 6 to 8 meters bgs (Figure 19).

Transect N Winter Survey

A 120 meter transect was completed approximately 85 meters upslope from the toe of the landslide mass on February 15, 2002 to compare seasonal variations of the radar signal. Transect N was a seasonal repeat of transect A. Surface material consisted of a mixture of coarse sand and gravel. The radargram display for this transect indicates a prominent reflector at approximately 6 to 8 meters below ground surface (bgs) similar to the previous radargram. An overall brightening of the signal is visible as compared to transect A. Where transect N crosses the south flank the prominent reflection loses

strength (Figure 20). A visual comparison of summer and winter surveys indicates an overall brightening of the winter survey (Figure 21).

Transect O Winter Survey

A 70 meter transect was completed approximately 140 meters upslope from the toe of the landslide mass on February 15, 2002 to compare seasonal variations of the radar signal. Transect O was a seasonal repeat of transect E. An overall brightening of the signal is visible as compared with transect E. Where transect O crosses the north flank this prominent reflection is still visible as compared with the September 07, 2002 survey (Figure 22). A visual comparison of the seasonal transects displays a high amplitude variation (Figure 23).

Eldon Transect Discussion

CMP survey results indicate a subsurface velocity of 0.129 m/ns. This value falls well within the range expected for dry sands and gravels (Table 1). Transects A through H all displayed a reflector at approximately 6 to 8 meters bgs. This reflector weakens where Transect A crosses the east flank and Transect E crosses the west flank of the disturbed landslide mass. Previous investigations by WSDOT (2000) have determined the slip surface to be located at approximately 6 to 15 meters bgs in glaciolacustrine silts and clays as previously described (Figure 6). These WSDOT findings of slip surface location were based on the shearing of installed wells during WSDOT monitoring.

Based on available information the prominent radargram reflectors are attributable to three possible subsurface conditions: 1) contact between outwash sand and gravels and the underlying glaciolacustrine silts and clays; 2) perched groundwater on glaciolacustrine

silts and clays; 3) disturbed soils, with resulting changes in their material properties, at landslide slip surface. Disturbed soils offer the most probable explanation for the cause of these prominent reflectors due to the loss of reflection strength near the respective east and west flanks of the landslide mass.

Winter transects display an overall “brightening” of the reflectors as compared with the late summer transects. This overall “brightening” can be attributed to an overall increase in the dielectric constant of the reflector and the seasonal change in water content within the vadose zone in this area of the landslide.

TAHUYA LANDSLIDE

Five GPR transects (I through M) using a 200 MHz antenna were completed on September 11, 2002, on various areas of the landslide (Figure 8). A common midpoint survey (CMP) was completed on October 26, 2002 using a 50 MHz antenna along transect I.

Tahuya Transect Results

CMP Survey

A hyperbolic reflection was seen at approximately 79 ns at 0.595 m of separation extending to 100 ns at 7.3 m of separation (Figure 24). Calculation of subsurface velocity using CMP surveys was completed as described. The CMP results indicate the average velocity of subsurface material to be 0.114 m/ns (Table 2). This average velocity was used for all subsurface units and specific velocities for each unit were not determined.

Transect I

A transect 55 meters in length was completed approximately 20 meters upslope from the toe of the landslide mass (Figure 8). Transect I was the longest and started near the right flank of the landslide mass. Surface material consisted of a mixture of coarse sand and gravel. The radargram display for this transect indicates various linear reflectors in the subsurface with a prominent positive amplitude reflection at approximately 7 meters bgs (Figure 25).

Transect J

A transect 15 meters in length was completed approximately 20 to 30 meters upslope from the toe of the landslide mass (Figure 8). Surface material consisted of a mixture of coarse sand and gravel. The radargram display for this transect indicates various linear reflectors in the subsurface with a prominent positive amplitude reflection at approximately 7 meters bgs (Figure 26).

Transect K

A transect 45 meters in length was completed approximately 30 meters upslope from the toe of the landslide mass (Figure 8). Surface material consisted of a mixture of coarse sand and gravel. The radargram display for this transect indicates a prominent positive amplitude reflection at approximately 7 meters bgs (Figure 27).

Transect L

A transect 20 meters in length was completed approximately 15 to 35 meters upslope from the toe of the landslide mass (Figure 8). Surface material consisted of a

mixture of coarse sand and gravel. The radargram display for this transect indicates a prominent positive amplitude reflection at approximately 7 meters bgs (Figure 28).

Transect M

A transect 30 meters in length was completed approximately 15 meters upslope from the toe of the landslide mass (Figure 8). Surface material consisted of a mixture of coarse sand and gravel. The radargram display for this transect indicates a prominent positive amplitude reflection at approximately 7 meters bgs (Figure 29).

Tahuya Transect Discussion

CMP survey results indicate a subsurface velocity of 0.114 m/ns. This value falls well within the range expected for materials predominantly consisting of silt (Table 1). The higher silt content effectively lowers the subsurface velocity as compared with sandy/gravel horizons.

Transects I through M all displayed a lack of internal reflectors until approximately 7 meters depth, where the radar signal was lost. The reflectors are not as prominent as the reflectors seen within the Eldon Landslide and are considered to highly attenuated and the radar signal is essentially lost due to highly conductive soils (Ekes and Hickin, 2001). Previous investigations by GeoEngineers (1998) have located a complex landslide mass with the primary slip surface (depth to reworked soils as described by GeoEngineers) located at approximately 7 meters bgs. These findings were based on borings completed on the site in April of 1998 by GeoEngineers (Figure 23).

DISCUSSION AND CONCLUSIONS

Transects A through H completed on the Eldon landslide all displayed a radar reflector at approximately 6 to 8 meters bgs. This reflector weakens where Transect A crosses the east flank and Transect E crosses the west flank of the disturbed landslide mass. Previous investigations by WSDOT (2000) have determined the slip surface to be located at approximately 6 to 15 meters bgs in glaciolacustrine silts and clays as previously described. Sands and gravels have been shown to have a lower dielectric constant and electrical conductivity resulting in a lower attenuation. This lower attenuation has a smaller effect on the radar signal as compared with silts and clays (Jol, 1989). Based on available information, prominent radargram reflectors located approximately 10 meters bgs can be attributed to three possible subsurface conditions: 1) contact between outwash sand and gravels and the underlying glaciolacustrine silts and clays; 2) perched groundwater on glaciolacustrine silts and clays; 3) disturbed soils at landslide slip surface. The weakened reflection at the flanks of the landslide mass in transects A and E suggests that these reflections are disturbed soils located at the landslide slip surface.

Transects N and O indicate that GPR can detect transient changes in material properties such as water content. Winter surveys display an overall increase in reflection amplitude of the reflected signal as compared to the late summer survey. Variations in the electrical properties of soils are usually associated with changes in volumetric water content which, in turn, give rise to radar reflections as previously noted (Davis and Annan, 1989). This change that is seen in the winter surveys indicates future work could

be done to correlate an increase in water content (as discussed further in Knight, 2001 and references therein), slip surface variation and landslide movement over time.

From the Tahuya slide, transects I through M all displayed a radar reflector at approximately 6 to 8 meters bgs. Previous investigations determined the slip surface to be located in the area of this study to be at approximately 7 meters bgs in loose sand, gravel, with occasional silty soil blocks. This description of source material containing “very hard silt” indicates a high probable silt fraction resulting in higher electrical conductivities resulting in a greater attenuation. This reflector that is seen at approximately 6 to 8 meters appears to be more of a weakened signal due to the suspected high conductivity of the soils.

The comparison between the Tahuya and Eldon radargram data presents the greatest insight into the limitations and strengths into the use of GPR on landslide slip surface delineation. What is imaged is largely determined by the variation of dielectric properties in the subsurface and the thickness of the resolvable layer. The range and resolution of GPR decreases with the presence of conductive materials like clays, silts or soils with conductive pore water (Davis and Annan, 1979).

The minimum detectable layer thickness (slip surface) and the accuracy with which the depth to a reflecting interface can be determined is dependent on the antennae wavelength and the properties of the sediment being measured (Jol 1995). Resolvable thickness, as a function of radar wave velocity and wavelength, for velocities between 0.10 m/ns and 0.15 m/ns using an antennae frequency of 200 MHz are 0.15 meters and 0.20 meters, respectively (Jol, 1995). This is best described as the thickness of a layer

decreases the power reflected decreases. The roughness of the interface between the two materials also affects the reflected signal power (Annan and Davis, 1977). Previous investigations did not determine the thickness of each of the landslide slip surfaces. This study determined that reflectors produced at the approximate location of the previously located Eldon landslide slip surface are a minimum thickness of 0.15 meters.

Based on this information GPR will not be effective on discrete, smooth landslide slip surfaces at depth, where there is attenuation due to highly conductive soils. For complex slip surfaces where the slip surface thickness is greater than 0.25 meters, less than 10 meters below ground surface, where low loss conditions exist, GPR with a 200 Mhz antennae can effectively be utilized to locate landslide slip surface as shown in this study.

CMP surveys only evaluated the velocity of the first overlying engineering geologic unit. Limitations exist with conversions of travel time and depth in complex stratigraphy and future studies should expand on underlying units and their velocities for appropriate scaling. Techniques (as described in Conyers and Goodman (1997)) such as stratigraphic correlations, transillumination methods and laboratory analyses of core samples should be further conducted to expand the knowledge of the electromagnetic properties of various subsurface materials. Further studies on landslide masses consisting of sand and gravel should be further conducted near the flanks and headscarp to attempt to view radargrams of subsurface features that propagate to the surface and provide additional information regarding GPR and its uses and limitations. Studies should also be conducted seasonally on landslide masses with installed piezometers to determine the

extent GPR can detect transient changes in water content and determine groundwater elevations within landslide masses.

Further studies in landslide slip surface characterization using GPR can provide cost effective techniques for slip surface determination in the geotechnical industry. December of 2003 geotechnical consultants charge from \$15,000 to \$50,000 to determine slip surface locations using proven methods (tiltmeters, inclinometers, extensometers and/or piezometers). Based on the geotechnical industries current hourly rates, a GPR survey can be conducted and evaluated for well under \$5,000 (excluding initial equipment investment which currently costs approximately \$30,000). Future studies combining techniques involving drilling, inclinometer installation and GPR surveys could provide a combination of cost effective technologies to characterize landslide slip surfaces. This combination of technologies could provide a large amount of data to be evaluated and correlated for proper landslide mitigation.

REFERENCES

- Annan, A.P. and Davis, J.L., 1977. Radar Range Analysis for Geological Materials. Report of Activities, Geological Survey of Canada, Paper 77-1B, p. 117-124.
- Babcock, R.S., Suczek, C.A., and Engebretson, D.C., 1994, The Crescent "Terrane", Olympic Peninsula and Southern Vancouver Island: Bulletin - State of Washington, Department of Natural Resources, Report: 80, p 141-157.s
- Barnhardt, W.A. and Kayen, R.E., 2000, Radar Structure of Earthquake-Induced, Coastal Landslides in Anchorage, Alaska: Environmental Geosciences, vol. 7, no.1, p. 38-45.
- Bruno, F. and Marillier, F., 2000, Test of High Resolution Seismic Reflection and Other Geophysical Techniques on the Boup Landslide in the Swiss Alps: Surveys in Geophysics, vol. 21, no. 4 p. 333-348.
- Conyers, L. and Goodman, D., 1997, Ground Penetrating Radar: An Introduction for Archeologists: Altamira Press, Walnut Creek, CA, 223 p.
- Davis, J.L. and Annan, A.P., 1989, Ground Penetrating Radar for High Resolution Mapping of Soil and Rock Stratigraphy: Geophysical Prospecting, v. 37, p. 531-551.
- Ekes, C. and Hickin, E.J., 2001, Ground Penetrating Radar Facies of the Paraglacial Cheekye Fan, Soutwestern British Columbia, Canada: Sedimentary Geology, v. 143, no.3-4, p. 199-217.
- GeoEngineers, 1998, Geotechnical Engineering Services, North Shore Landslide Evaluation, Tahuya, Washington. 15 p.
- Grasmuck, M., and Green, A., 1996, 3-D Georadar Mapping: Looking Into the Subsurface: Environmental and Engineering Geoscience, v. II, no. 2, p. 195-200.
- Holtz, R.D. and Schuster, R.L., 1996, Stabilization of Soil Slopes. Landslides: Investigation and Mitigation: Transportation Research Board, Special Report 247, p. 439-473.
- Hruska, J., and Hubatka, F., 2000, Landslides Investigation and Monitoring by a High Performance Ground Penetrating Radar System: Proceedings of the Eighth International Conference on Ground Penetrating Radar, SPIE, v. 4084, p. 688- 693.
- Jol, H.M., 1995, Ground Penetrating Radar Antennae Frequencies and Transmitter Powers Compared for Penetration, Depth, Resolution and Reflection Continuity: Geophysical Prospecting, v. 43, p. 693-709.

Jol, H.M. and Junck, M.B., 2000, High Resolution Ground Penetrating Radar Imaging (225-900Mhz) of Geomorphic and Geologic Settings: Examples From Utah, Washington and Wisconsin: Proceedings of the Eighth International Conference on Ground Penetrating Radar SPIE, v. 4084, p. 69-79.

Knight, R., 2001, Ground Penetrating Radar for Environmental Applications: Annual Review Earth Planet Science, v. 29, p. 229-255.

Mikkelsen, P.E., 1996, Field Instrumentation. Landslides: Investigation and Mitigation: Transportation Research Board, Special Report 247, p. 278-316.

Olhoeft, G.R., 1981, Physical Properties of Rocks and Minerals: McGraw Hill, New York. p. 257-330.

Sellman, P.V., Arcone S.S., and Delaney A.J., 1983, Radar Profiling of Buried Reflectors and the Groundwater Table: Cold Regions Research and Engineering Laboratory Report 83-11, p. 1-10.

Schuster, R.L., 1996, Socioeconomic Significance of Landslides. Landslides: Investigation and Mitigation: Transportation Research Board, Special Report 247, p. 12-31

Topp, G.C., Davis, J.L. and Annan, A.P., 1980, Electromagnetic Determination of Soil Water Content: Measurements in Coaxial Transmission Lines: Water Resources Research, no. 16, v.3., p. 574-582.

Ulrickson, C.P.F., 1982, Application of Impulse Radar to Civil Engineering [PH.D. thesis]: University of Technology, Lund, Sweden, 173 p.

Walden, A.T., and Hosken, W.J., 1985, An Investigation of the Spectral Properties of Primary Reflection Coefficients: Geophysical Prospecting, v. 33, p.400-435.

Washington State Department of Transportation, 2000, Eldon Landslide, Geotechnical Study of the Eldon Vicinity Landslide Adjacent to Hood Canal, Final Geotechnical Report, 9 p.

TABLE 1
TYPICAL DIELECTRIC CONSTANT, ELECTRICAL CONDUCTIVITY AND
VELOCITY OBSERVED IN COMMON GEOLOGICAL MATERIALS^a

Material	K	σ (mS/m)	V (m/ns)
Air	1	0	0.3
Distilled Water	80	0.01	0.033
Fresh Water	80	0.5	0.033
Sea Water	80	30000	0.01
Dry Sand	3 - 5	0.01	0.15
Saturated Sand	20 - 30	0.1 - 1.0	0.06
Limestone	4 - 8	0.5 - 2	0.12
Shales	5 - 15	1 - 100	0.09
Silts	5 - 30	1 - 100	0.07
Clays	5 - 40	2 - 1000	0.06
Granite	4 - 6	0.01 - 1	0.13
Dry Salt	5 - 6	0.01 - 1	0.13
Ice	3 - 4	0.01	0.16

Notes:
^a Adapted from Davis and Annan 1989
K - Dielectric Constant
 σ - Electrical Conductivity
V - Velocity
 $V = c/(K)^{1/2}$ where c is 3×10^8 m/s (Knight, 2001)

TABLE 2
COMMON MIDPOINT SURVEY^a

ELDON LANDSLIDE			
T (ns)	D (m)	T (ns) ^d	D (m) ^e
90	3.24	8100	10.4976
96	6.21	9216	38.5641
109	8.91	11881	79.3881
121	11.61	14641	134.7921
140	14.31	19600	204.7761
SLOPE^f = 0.0168 VELOCITY^g = 0.129 m/ns			

TAHUYA LANDSLIDE			
T (ns)	D (m)	T (ns) ^d	D (m) ^e
79	0.595	6241	0.354025
79	1.98	6241	3.9204
87.4	4.74	7638.76	22.4676
100	7.13	10000	50.8369
--	--	--	--
SLOPE^f = 0.013 VELOCITY^g = 0.114 m/ns			

Notes:

T- time

D - distance

^a As described in Davis and Annan 1977

^b Figure 11.

^c Figure 24.

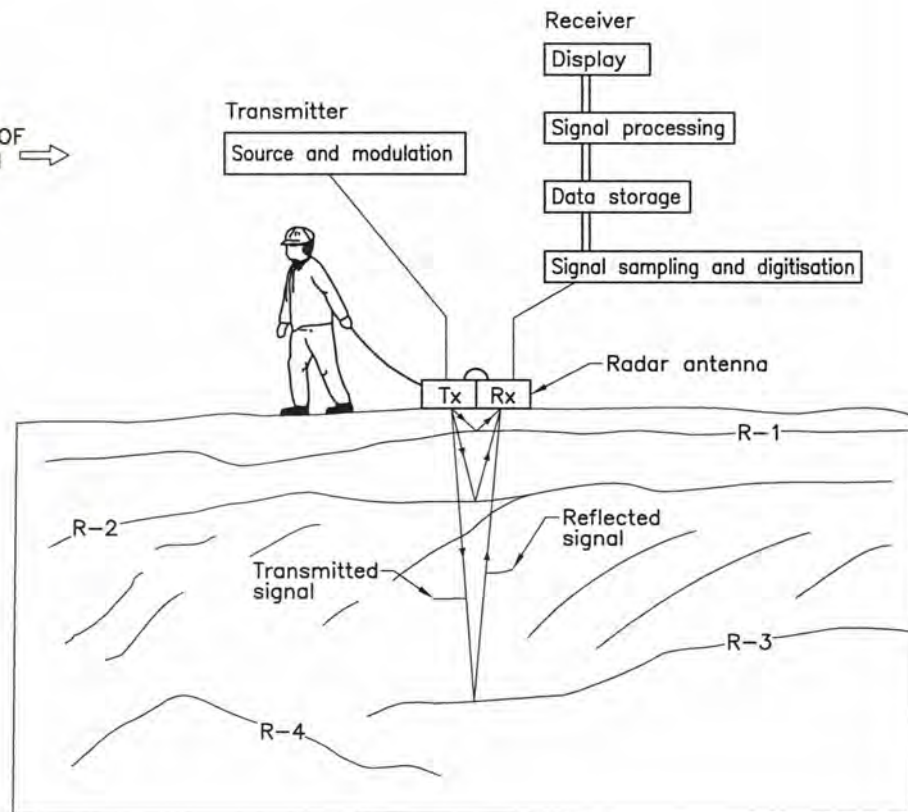
^d (time)² from hyperbola

^e (distance)² from hyperbola

^f distance/time

^g Gradient of the slope is equal to Velocity^{1/2}

(A) COMPONENTS OF RADAR SYSTEM →



Simplified diagram of (A) the constituents of a radar system with the interpreted section of adapted from Butler et al. (1991) and Daniels et al. (1988) (Reynolds, 1997).

NOT TO SCALE

SIMPLIFIED DIAGRAM SHOWING COMPONENTS OF GPR SYSTEM

FIGURE 1

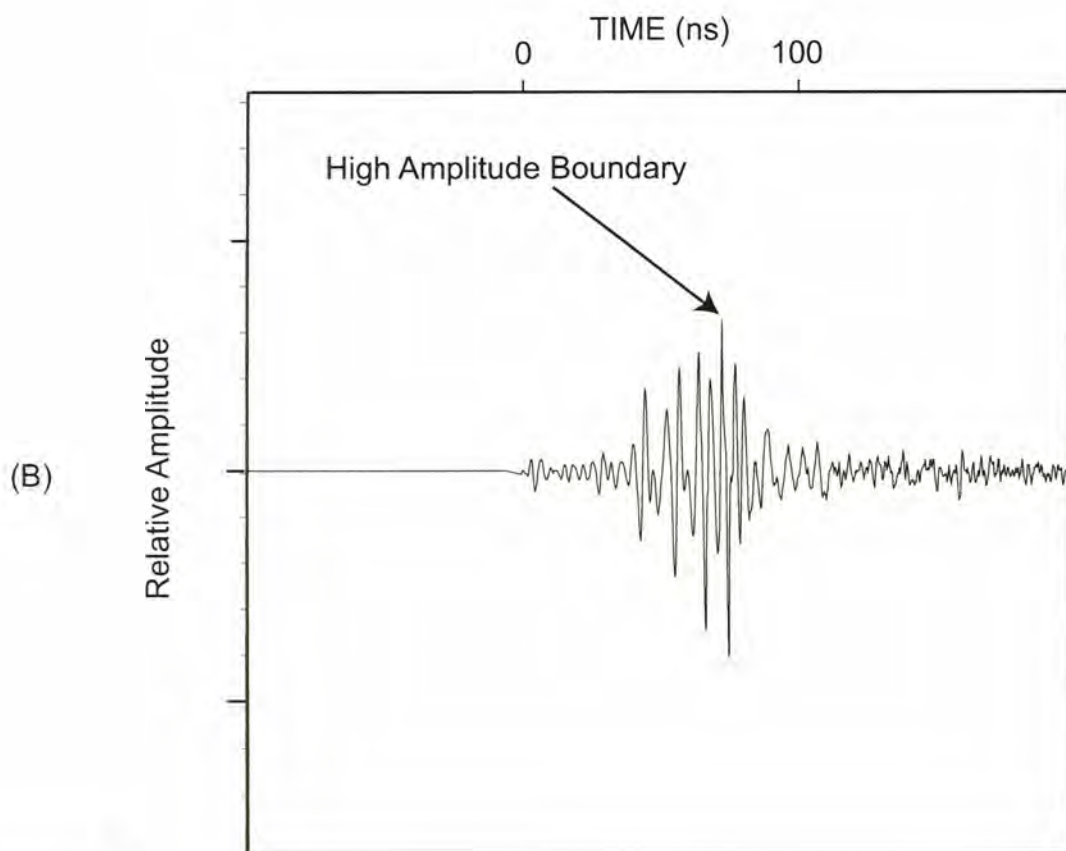
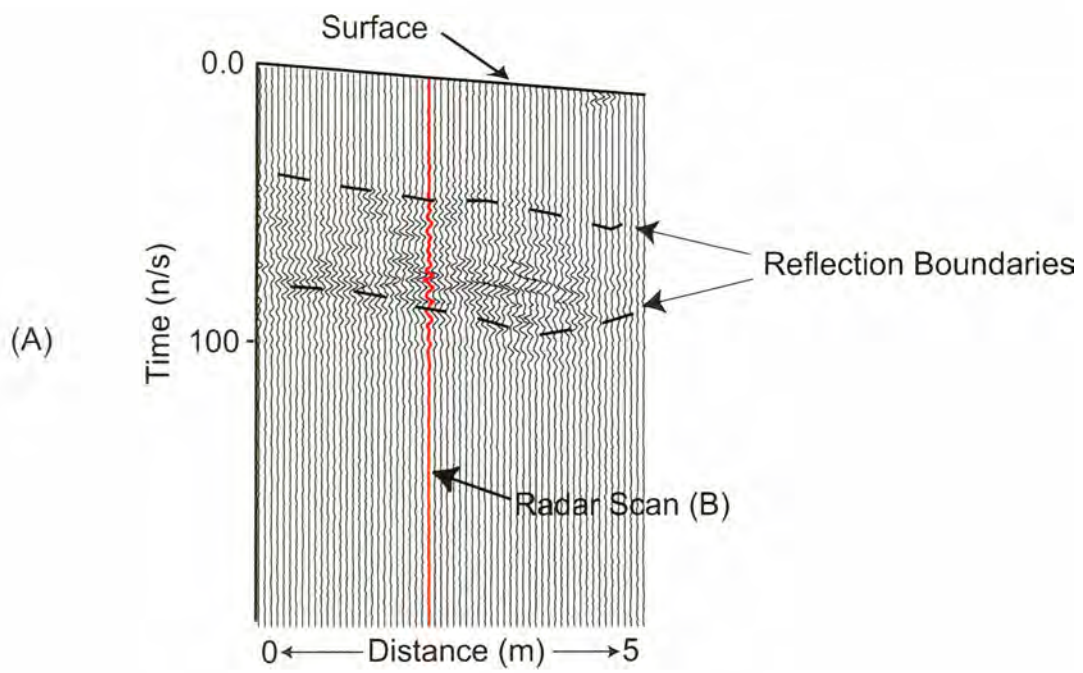
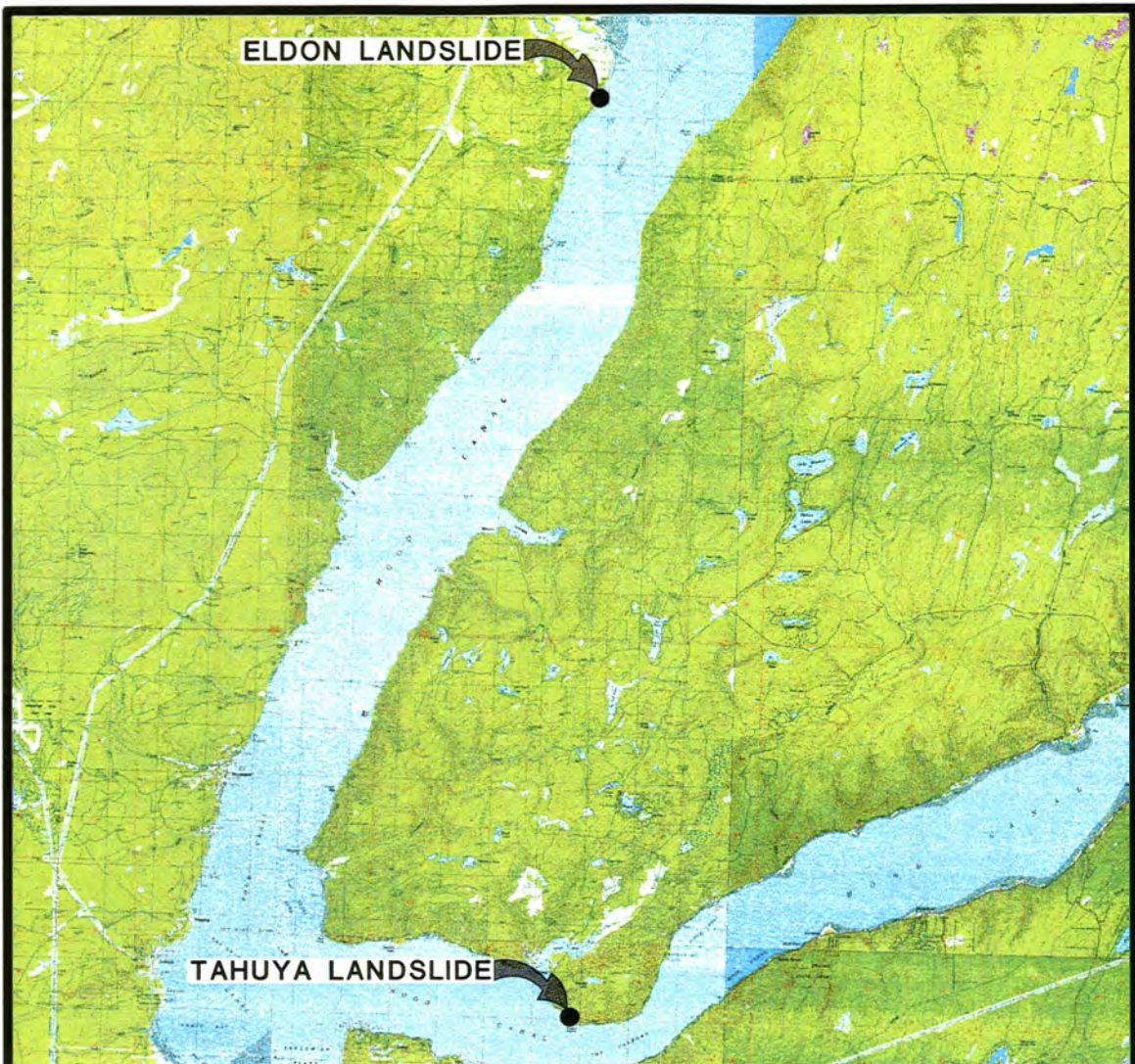


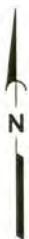
Figure 2. (A) Typical radargram displayed as a linscan (B) Oscilloscope trace of single radar scan as highlighted in radargram.



Data Source: Topography from Sure!Maps at scale of 1:24k.

All locations are approximate.

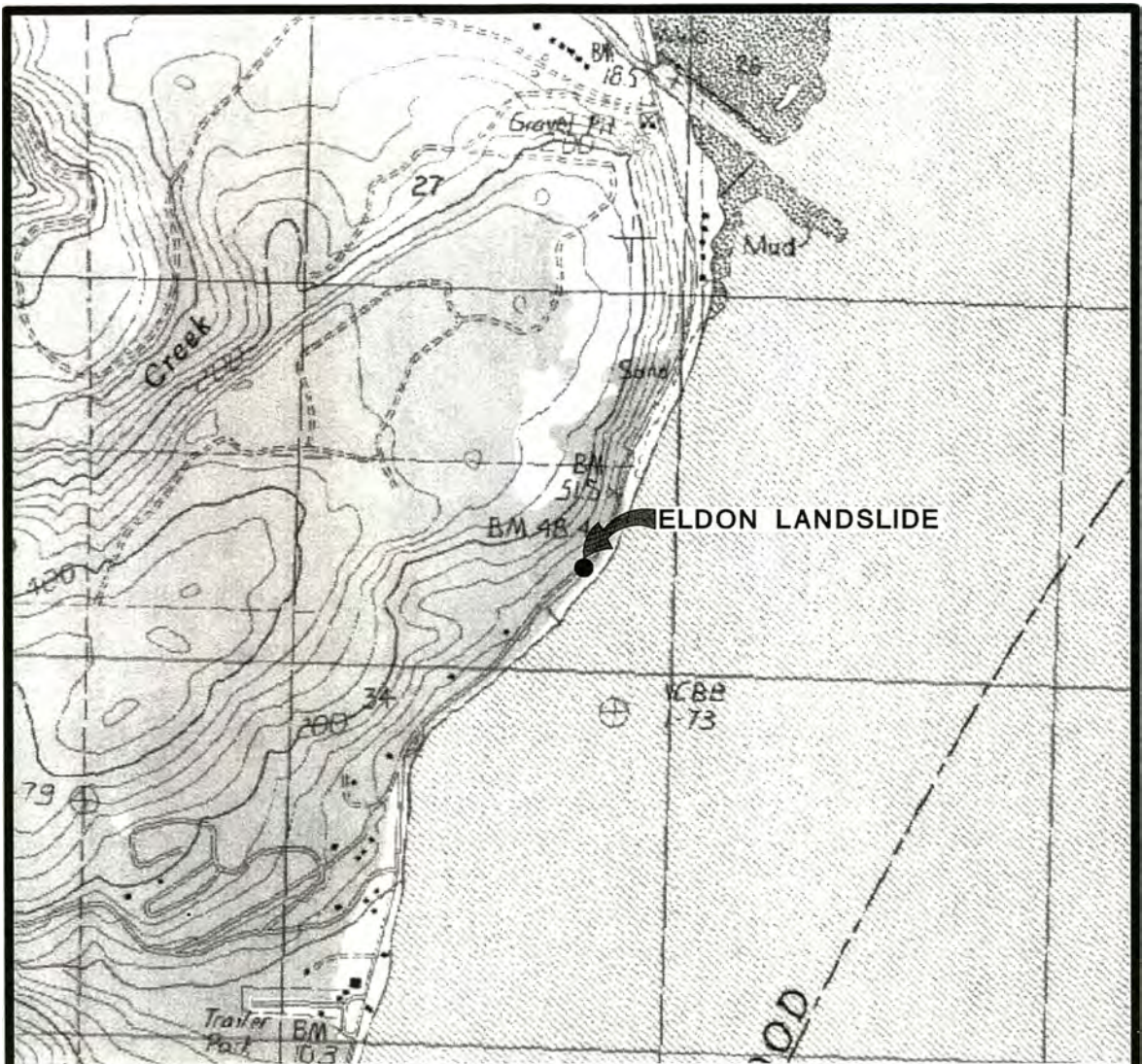
Lambert Conformal Conic
 Washington State Plane South
 North American Datum 1983



NOT TO SCALE

**LOCATION OF ELDON AND TAHUYA
 LANDSLIDES IN WASHINGTON STATE**

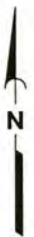
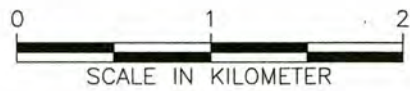
FIGURE 3



Data Source: Topography from Sure!Maps at scale of 1:24k.

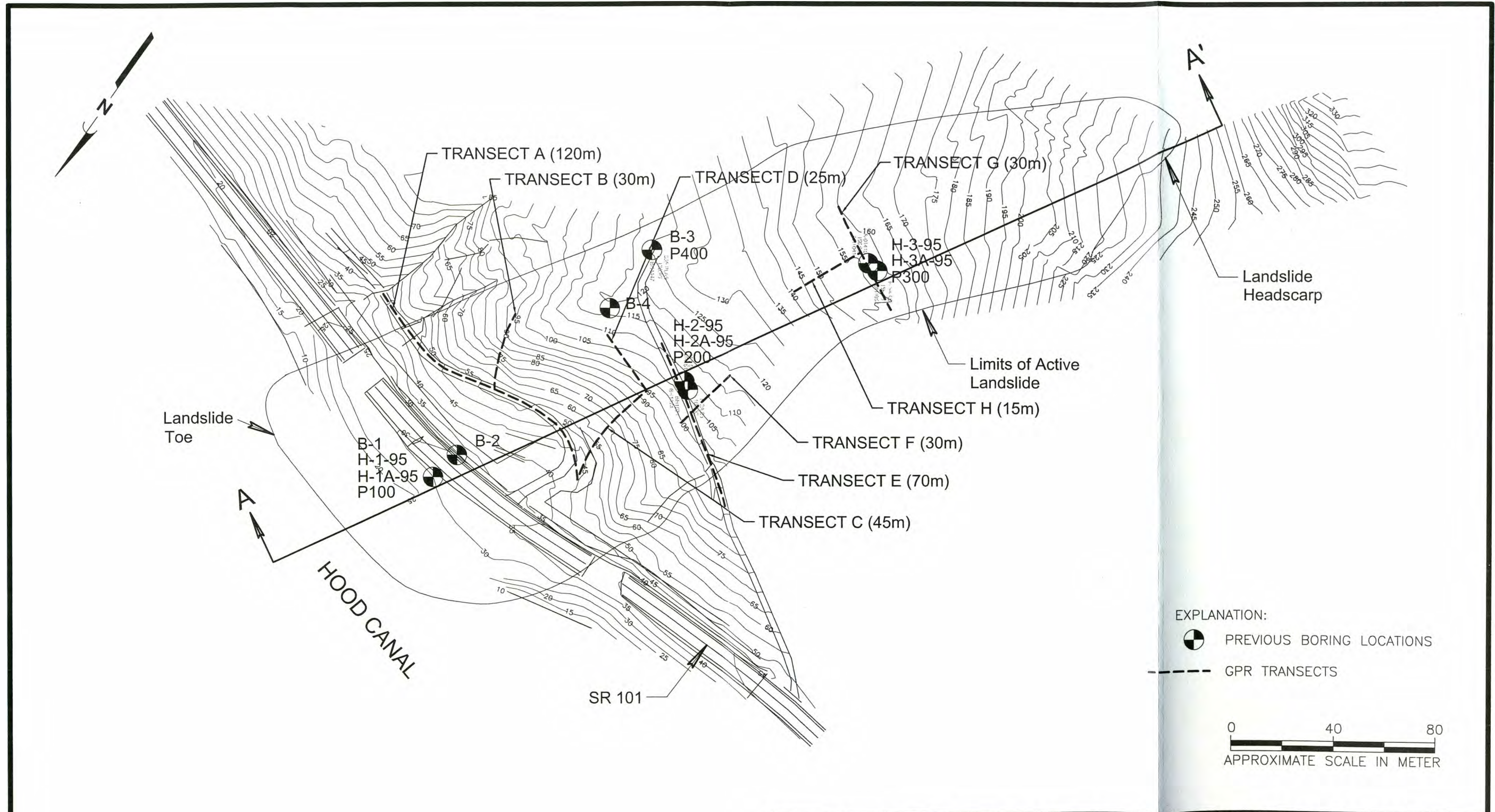
All locations are approximate.

Lambert Conformal Conic
 Washington State Plane South
 North American Datum 1983



LOCATION OF ELDON LANDSLIDE

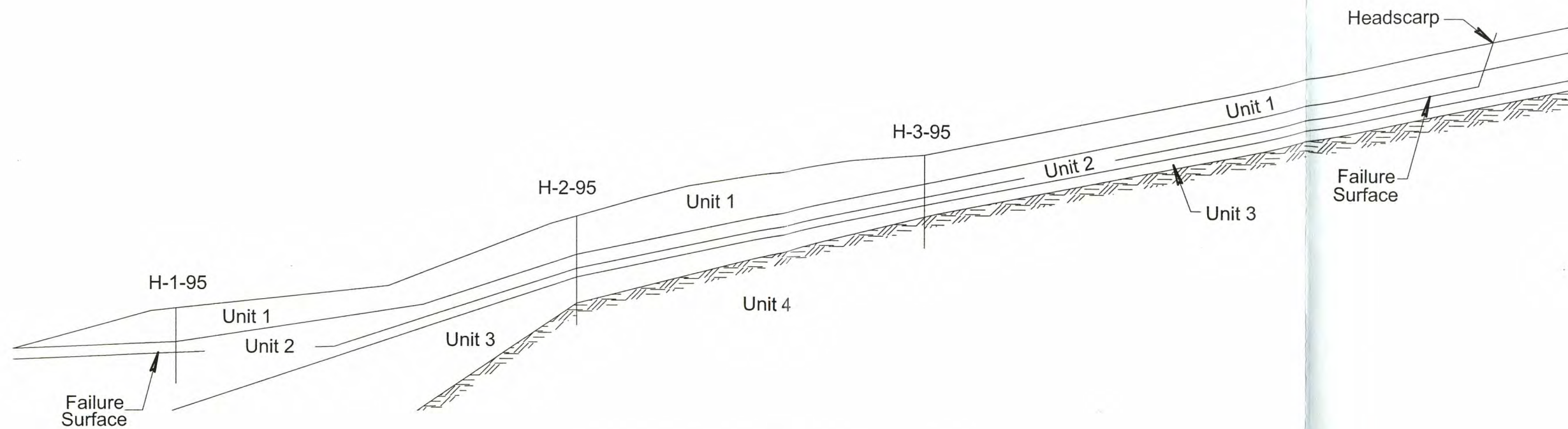
FIGURE 4



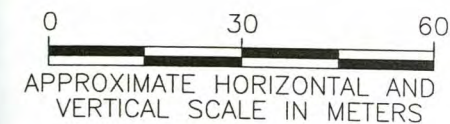
ELDON LANDSLIDE FEATURES SHOWING HEADSCARP, TOE AND RESPECTIVE FLANKS. GPR TRANSECTS A THROUGH G COMPLETED AS SHOWN ON MAP.

FIGURE 5

Reference: Base drawing provided by WSDOT, 04/14/00.



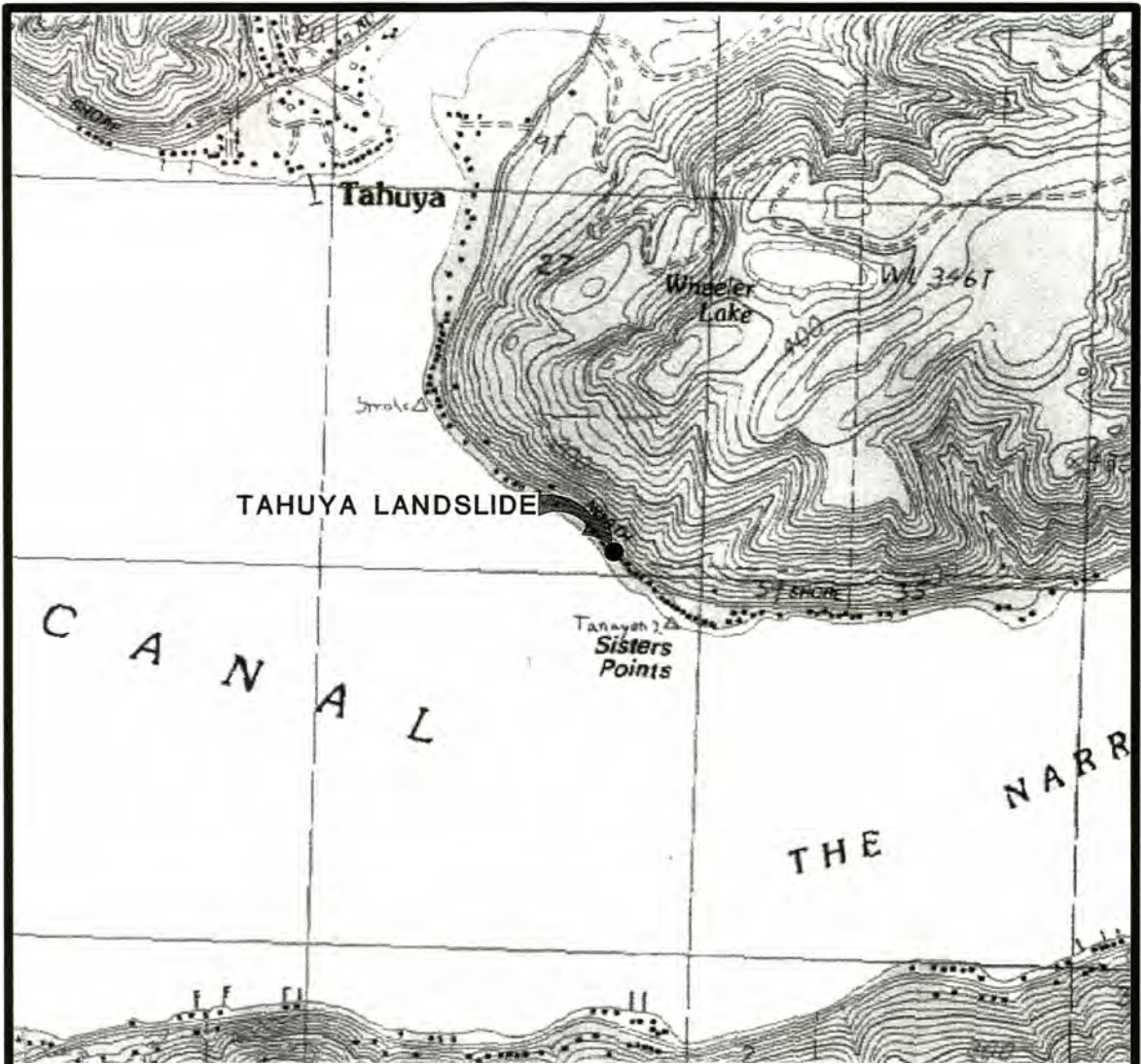
- Unit 1 Outwash Sand and Gravel
- Unit 2 Glacio-lucustrine Silt and Clay
- Unit 3 Glacial Till
- Unit 4 Basalt Bedrock



**GEOLOGIC CROSS SECTION A-A' OF
ELDON LANDSLIDE**

FIGURE 6

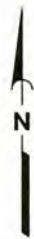
Reference: Base drawing provided by WSDOT, 04/14/00.



Data Source: Topography from Sure!Maps at scale of 1:24k.

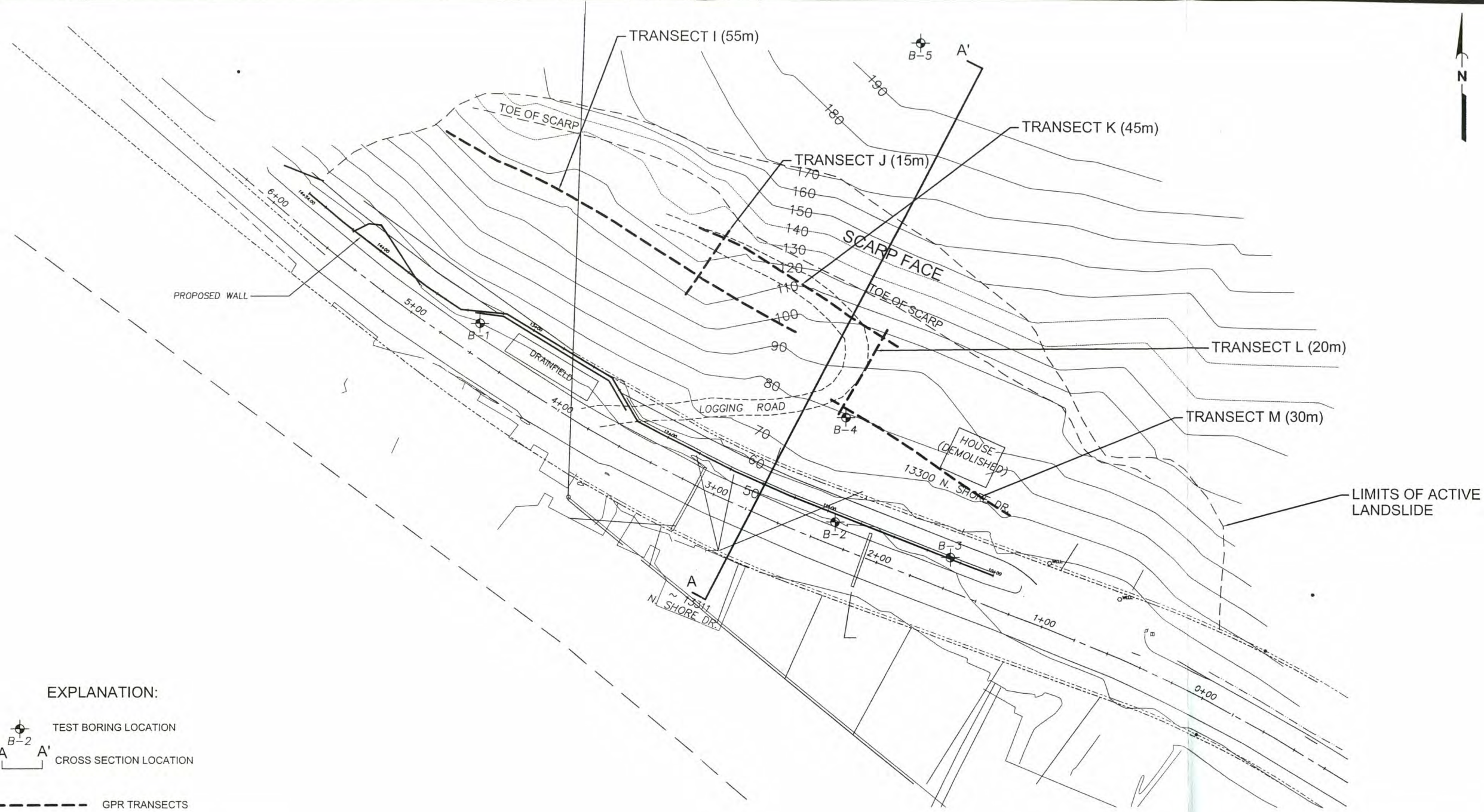
All locations are approximate.

Lambert Conformal Conic
 Washington State Plane South
 North American Datum 1983



LOCATION OF TAHUYA LANDSLIDE

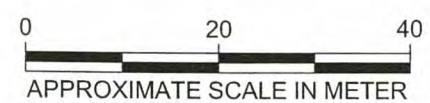
FIGURE 7



EXPLANATION:

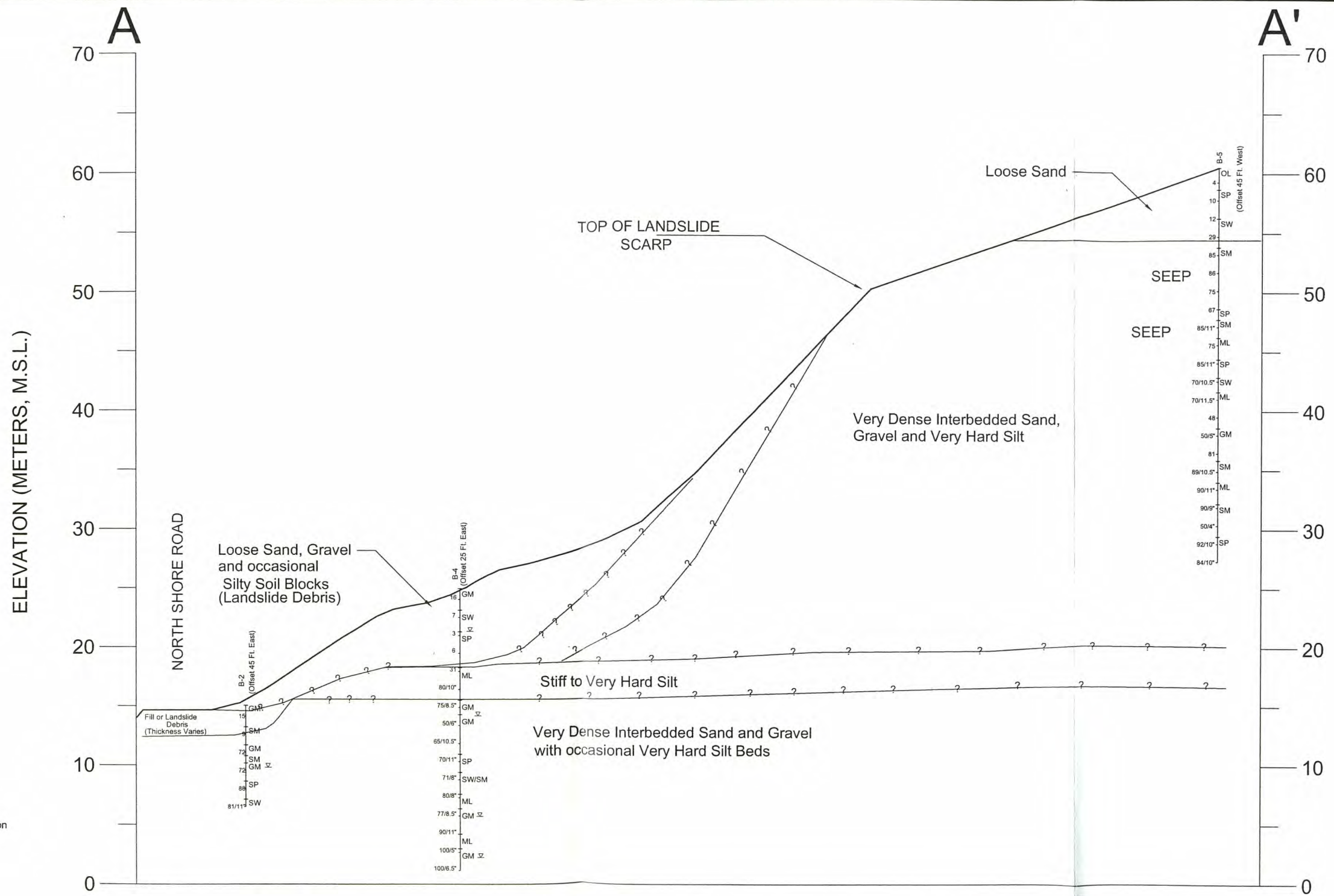
- TEST BORING LOCATION
- CROSS SECTION LOCATION
- GPR TRANSECTS

Note: The locations of all features shown are approximate.
 Reference: Drawing entitled "North Shore Slide" by Mason County Engineers, 06/18/97.

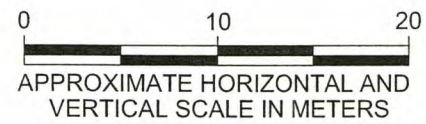


TAHUYA LANDSLIDE FEATURES SHOWING HEADSCARP, TOE AND RESPECTIVE FLANKS. GPR TRANSECTS I THROUGH M COMPLETED AS SHOWN ON MAP.

FIGURE 8

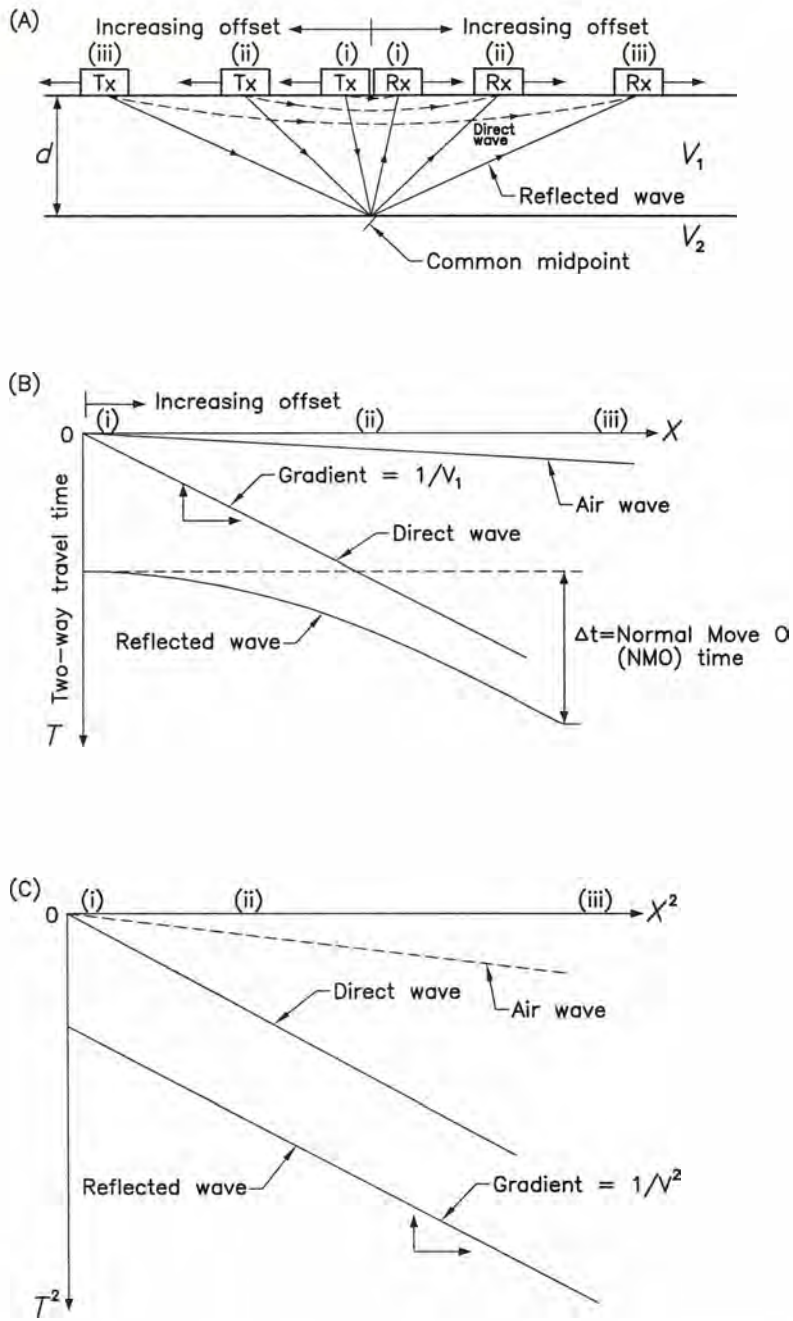


Note: The locations of all features shown are approximate.
Reference: GeoEngineers 09/09/98.



GEOLOGIC CROSS SECTION A-A' OF TAHUYA LANDSLIDE

FIGURE 9



(A) CMP sounding with (B) a time-distance ($T-X$) graph with normal movement and (C) the corresponding T^2-X^2 graph (Reynolds, 1997).

NOT TO SCALE

**SIMPLIFIED CMP SOUNDING WITH
TIME-DISTANCE GRAPH**

FIGURE 10

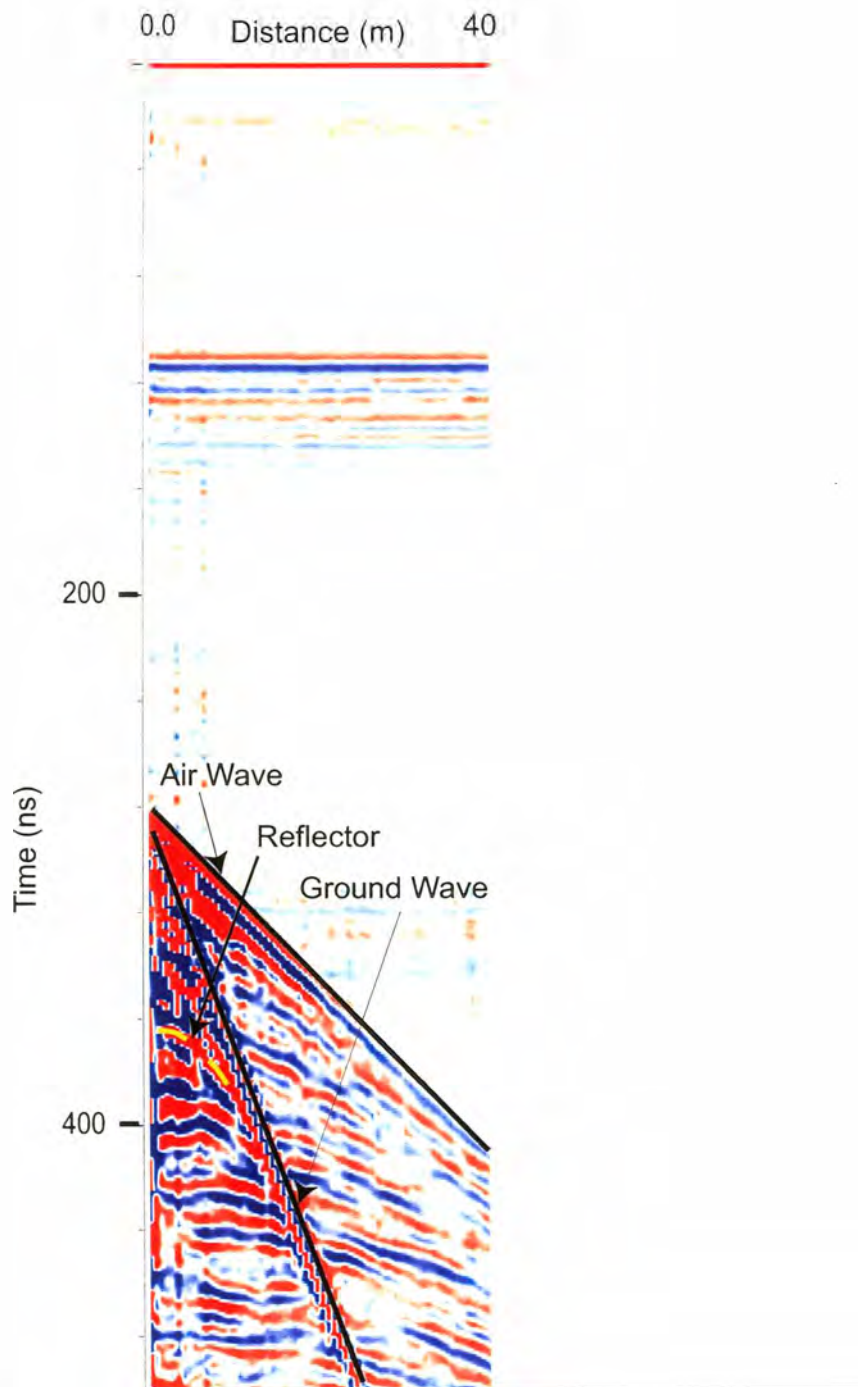


Figure 11. CMP survey results for Eldon Landslide along Transect E. (see Table 2 for distance versus time for reflector).

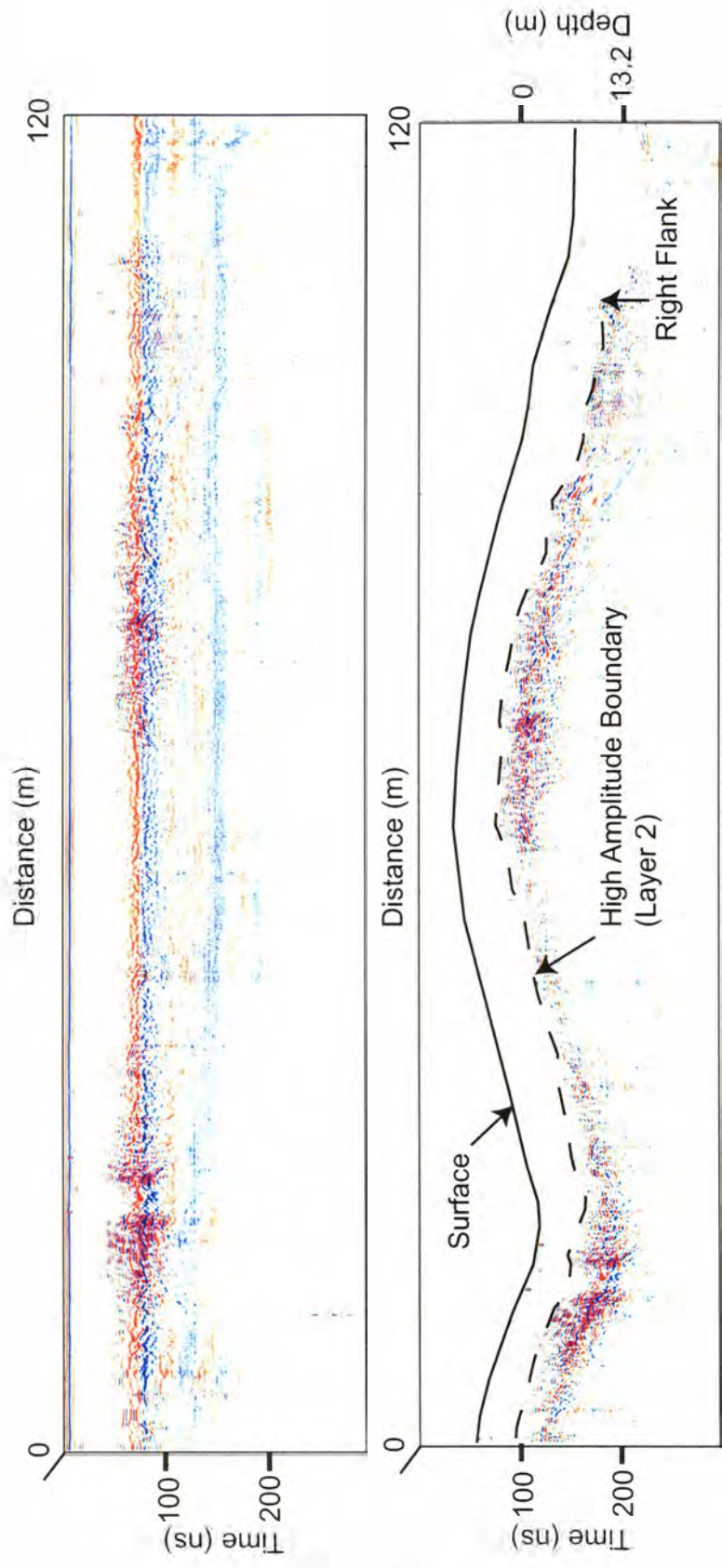


Figure 12. Transect A, Eldon Landslide; raw (top) and processed (bottom) data corrected for elevation with radar features noted.

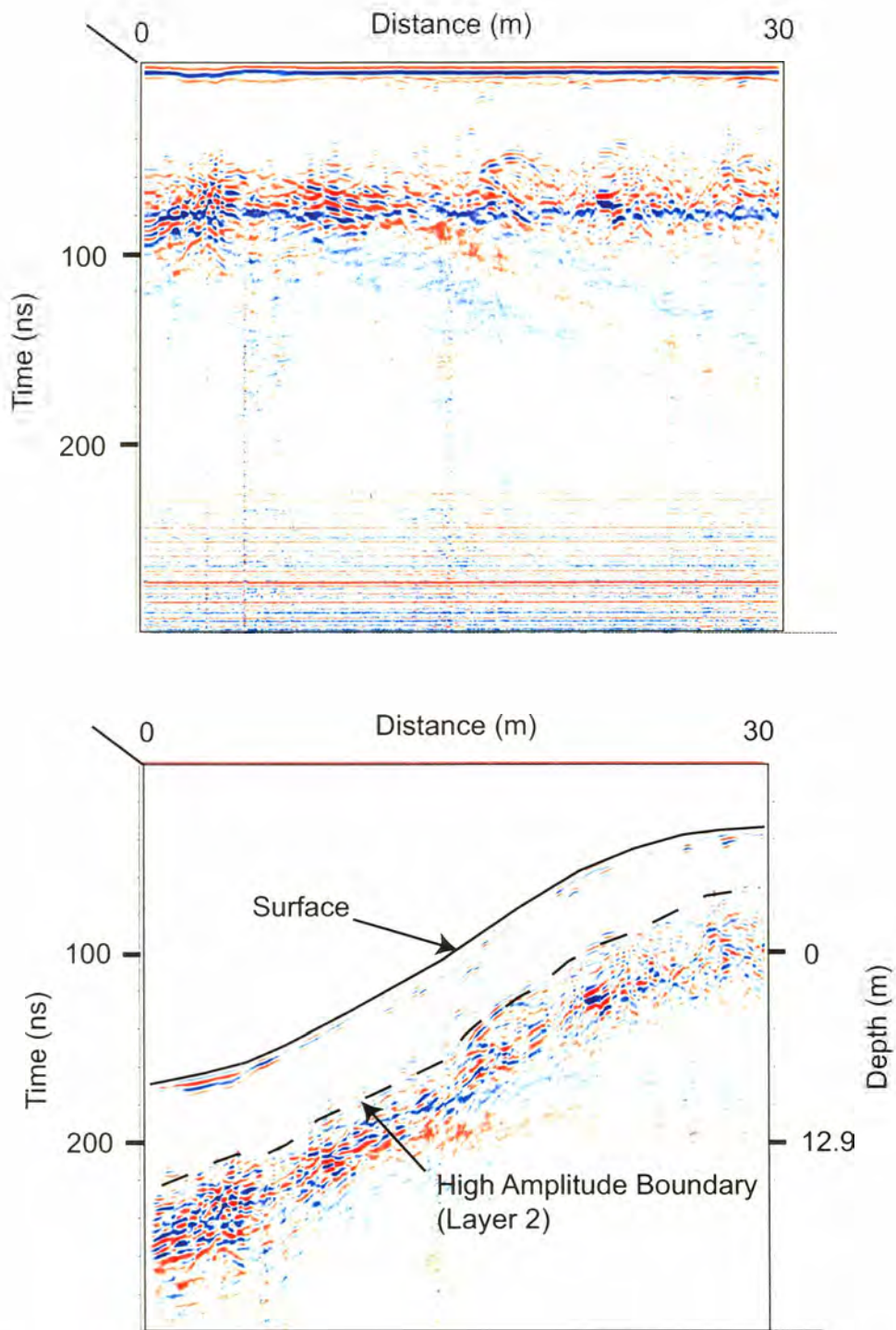


Figure 13. Transect B, Eldon Landslide; raw (top) and processed (bottom) data corrected for elevation with radar features noted.

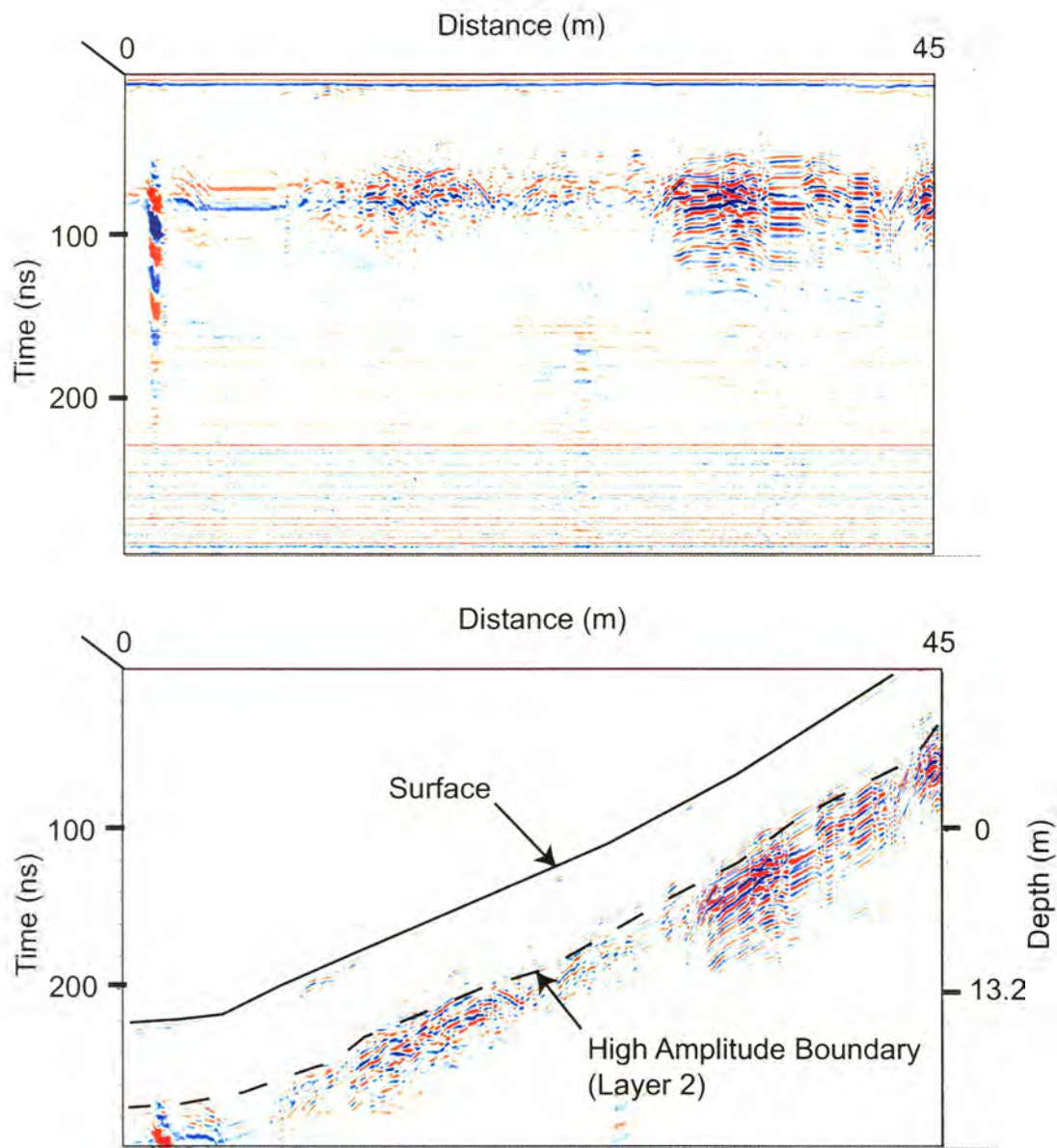


Figure 14. Transect C, Eldon Landslide; raw (top) and processed (bottom) data corrected for elevation with radar features noted.

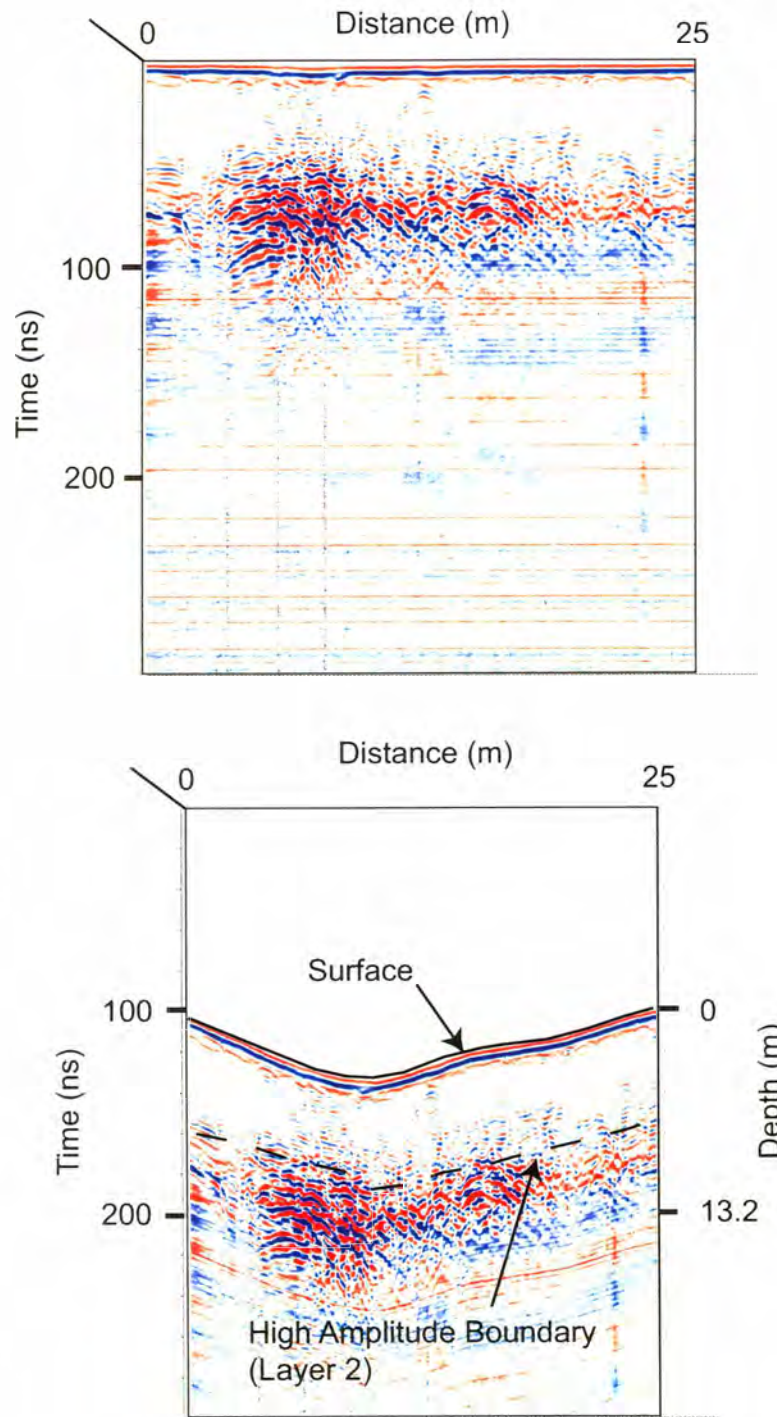


Figure 15. Transect D, Eldon Landslide; raw (top) and processed (bottom) data corrected for elevation with radar features noted.

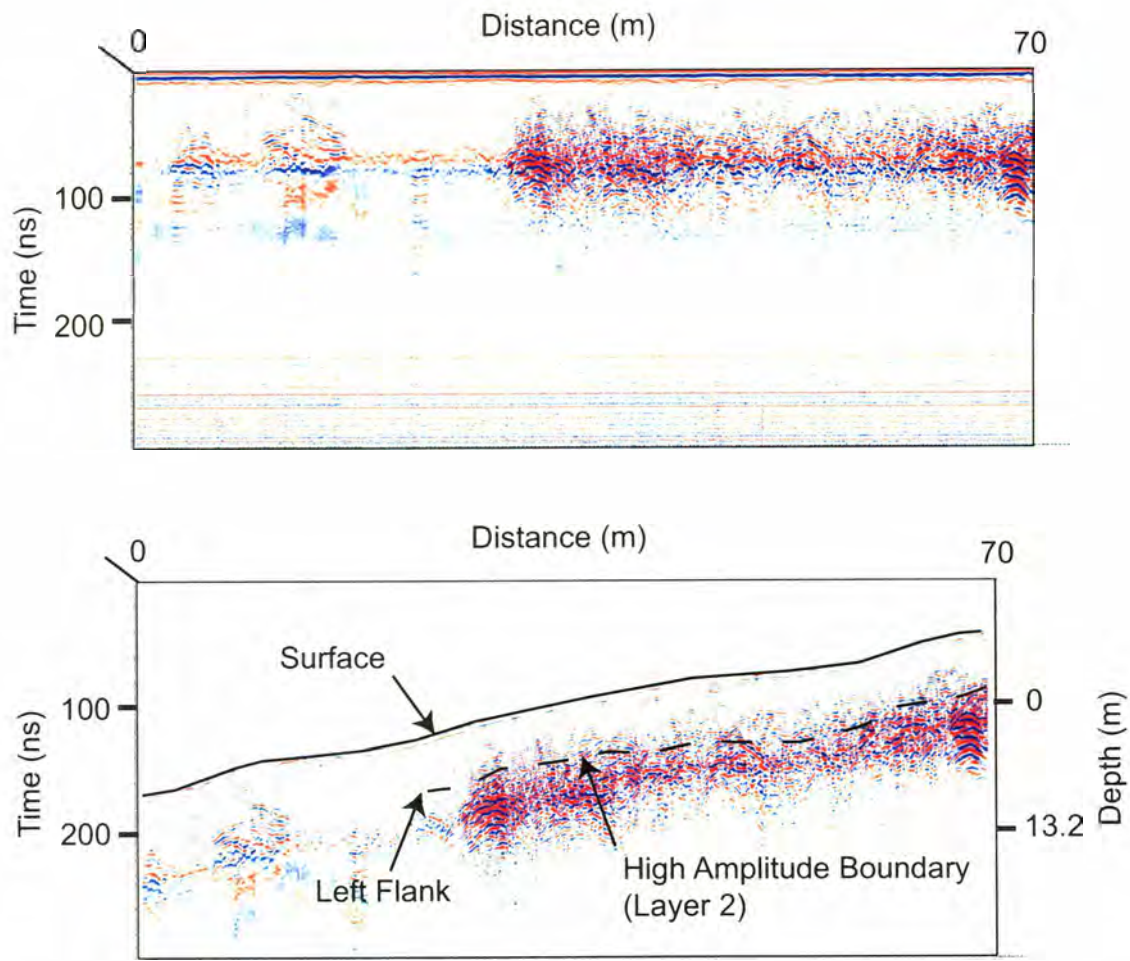


Figure 16. Transect E, Eldon Landslide; raw (top) and processed (bottom) data corrected for elevation with radar features noted.

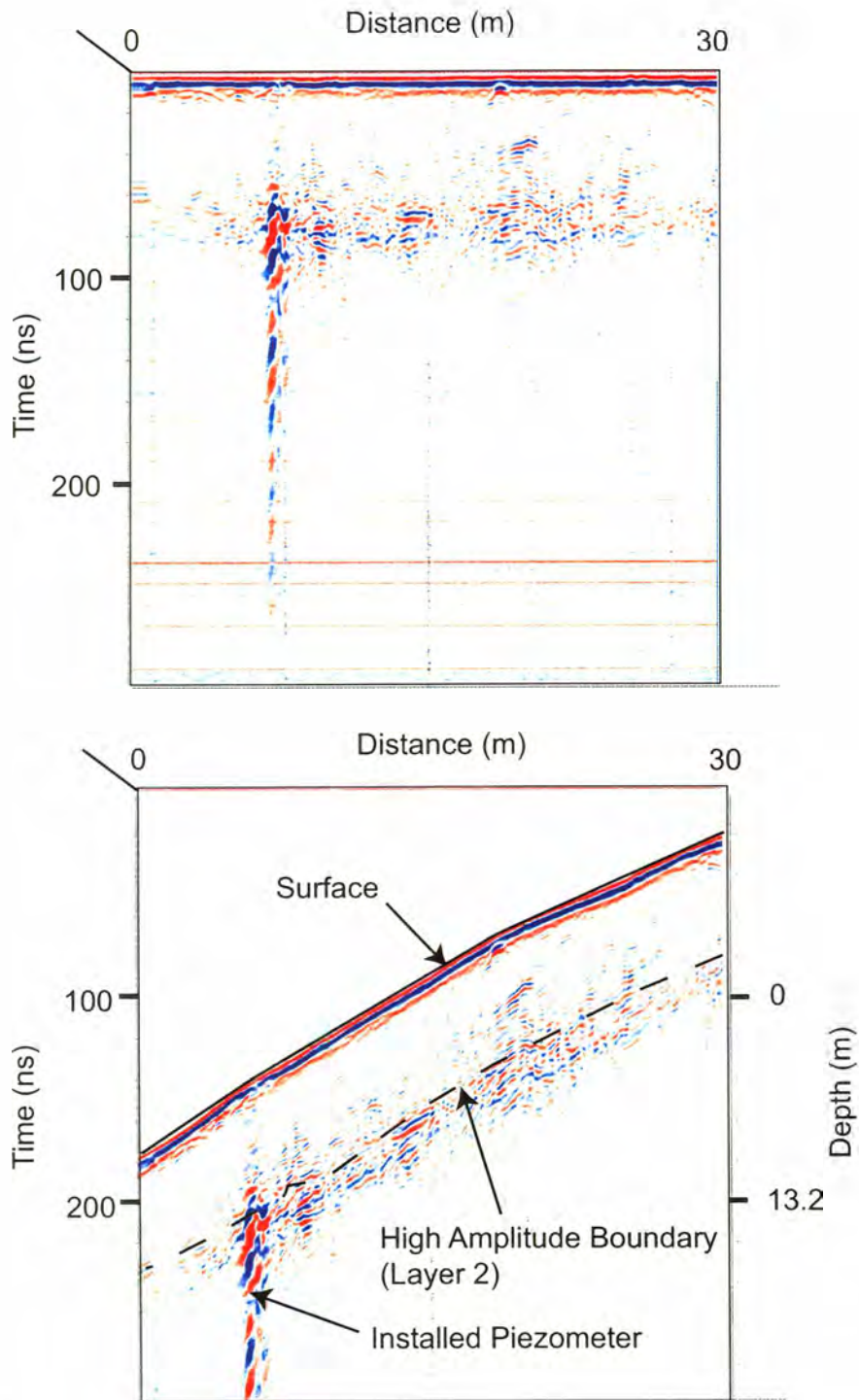


Figure 17. Transect F, Eldon Landslide; raw (top) and processed (bottom) data corrected for elevation with radar features noted.

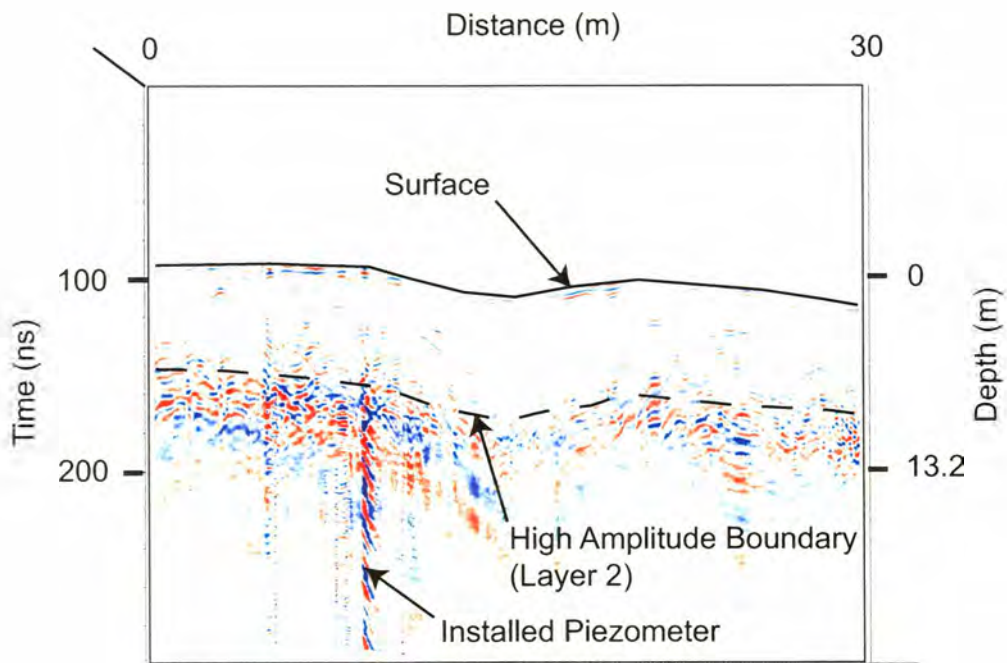
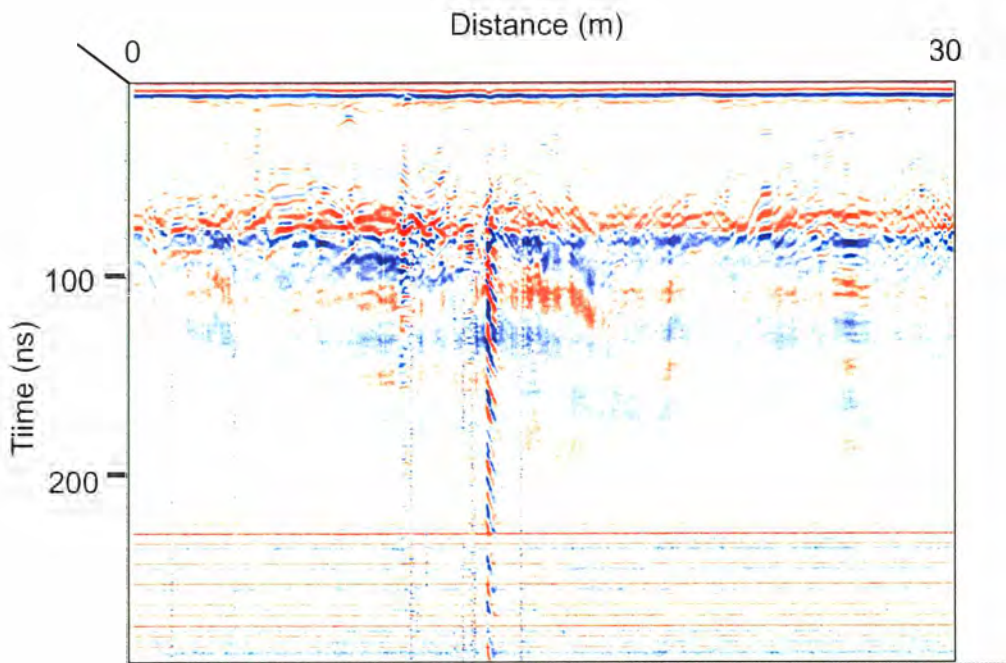


Figure 18. Transect G, Eldon Landslide; raw (top) and processed (bottom) data corrected for elevation with radar features noted.

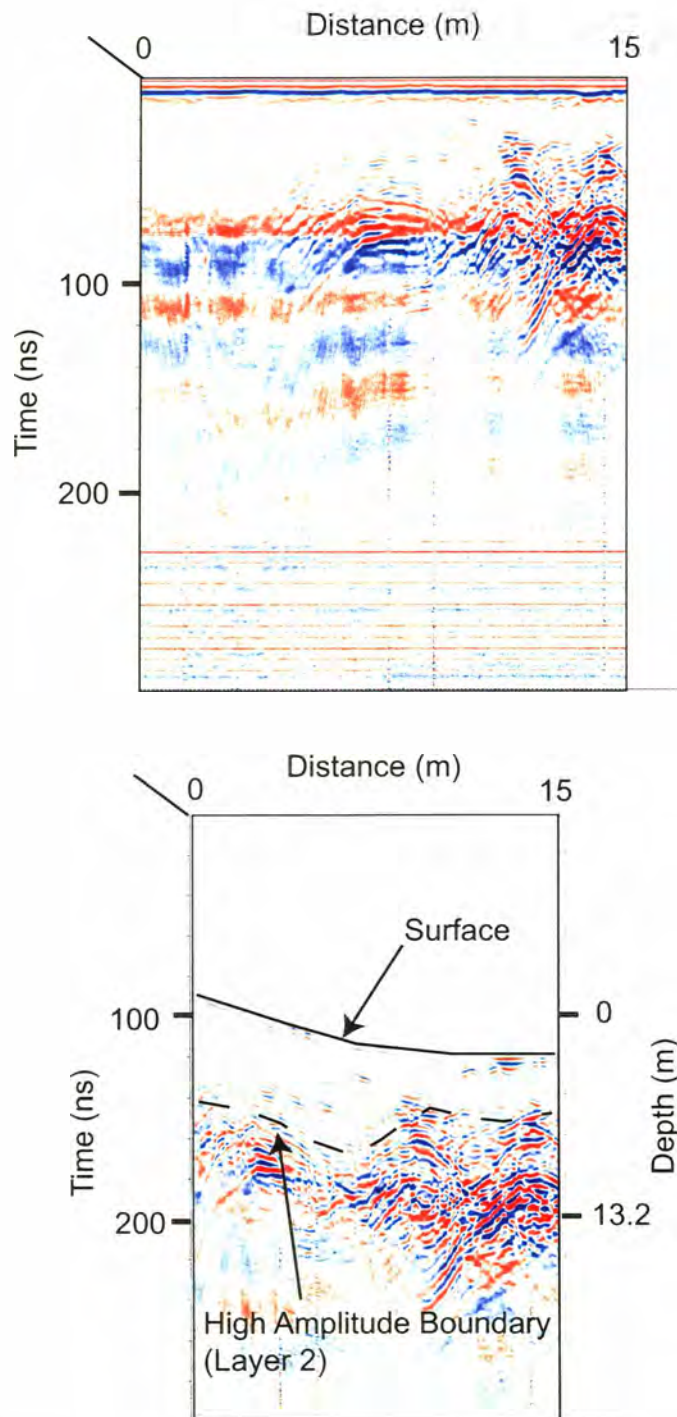


Figure 19. Transect H, Eldon Landslide; raw (top) and processed (bottom) data corrected for elevation with radar features noted.

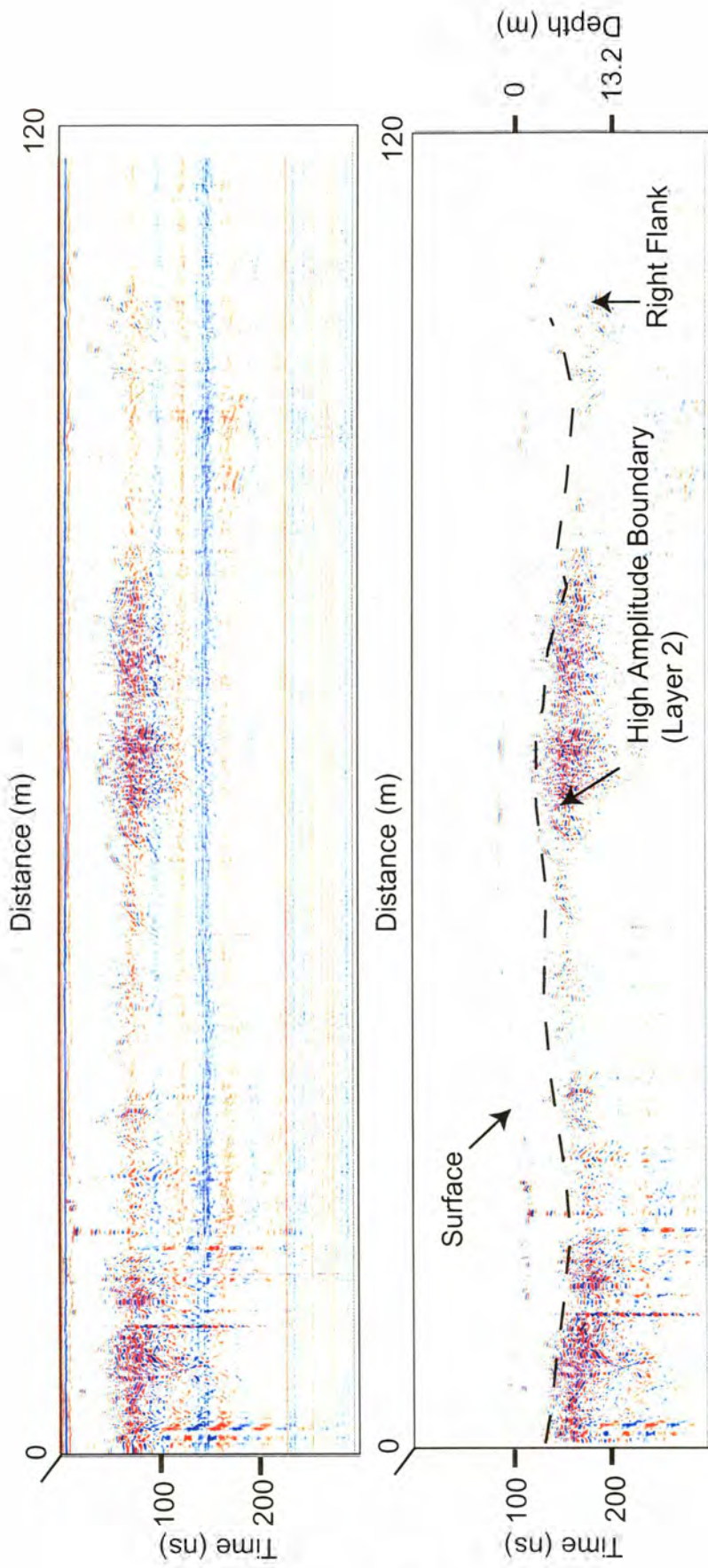


Figure 20. Transect N, Eldon Landslide; raw (top) and processed (bottom) data corrected for elevation with radar features noted.

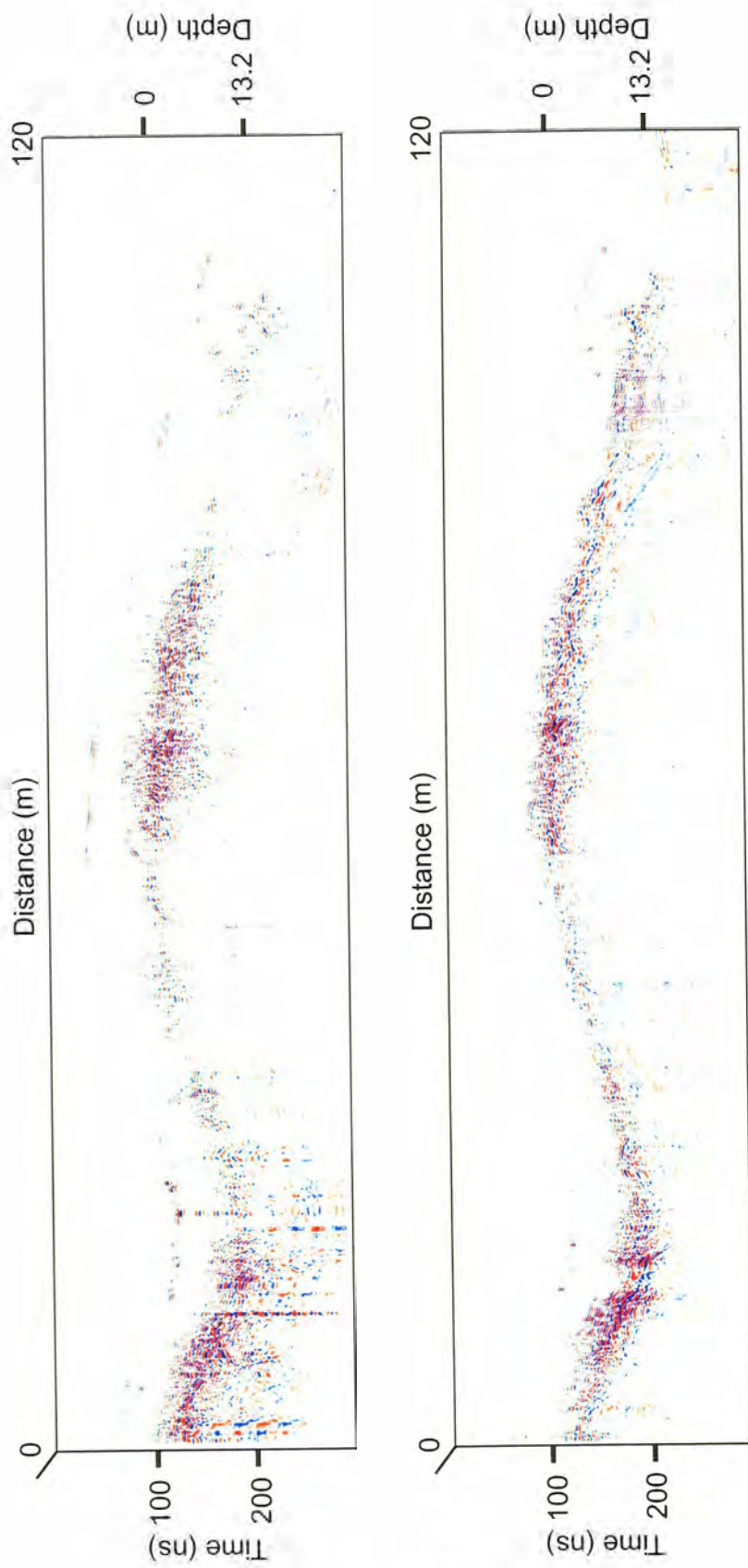


Figure 21. Transect N (top) and transect A (bottom) data corrected for elevation with radar features noted. Slight brightening of radar image in winter months (top).

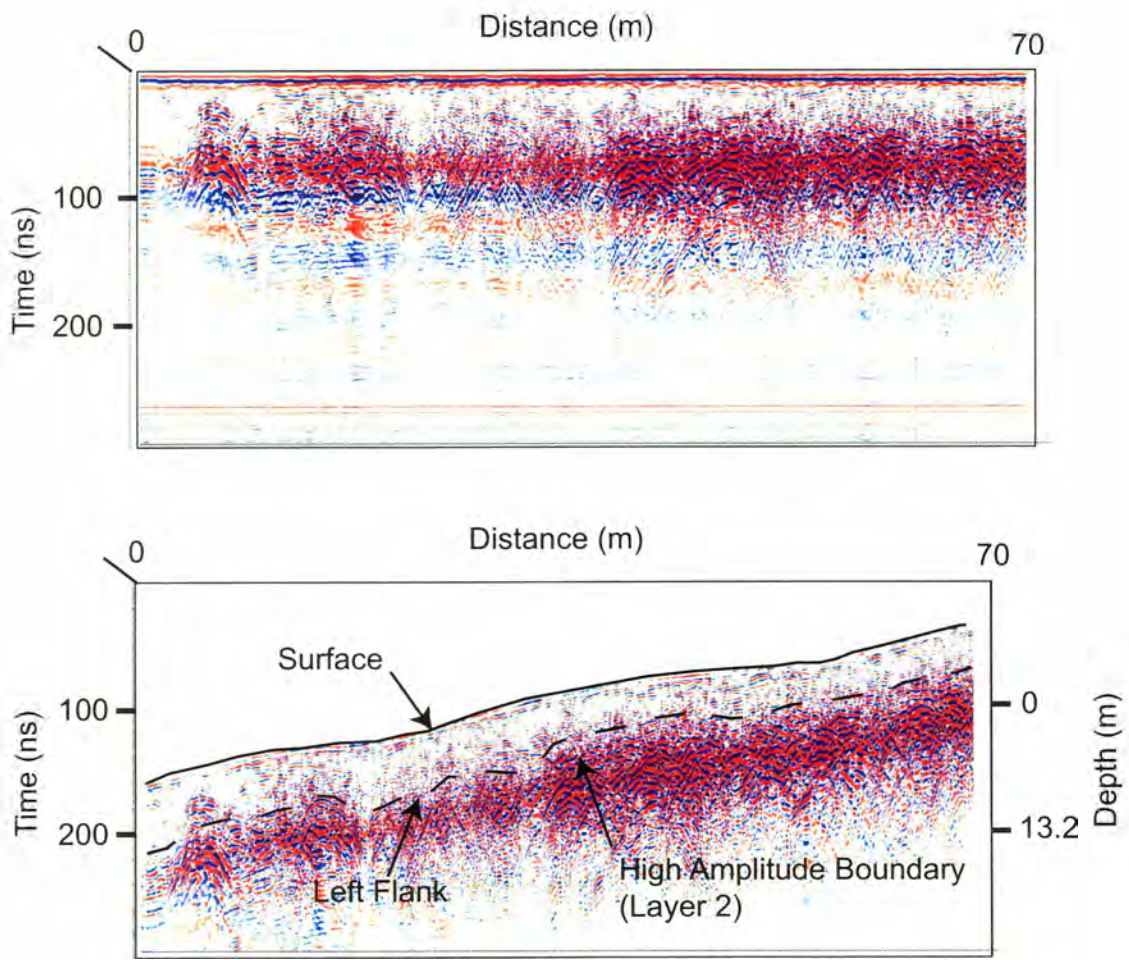


Figure 22. Transect O, Eldon Landslide; raw (top) and processed (bottom) data corrected for elevation with radar features noted.

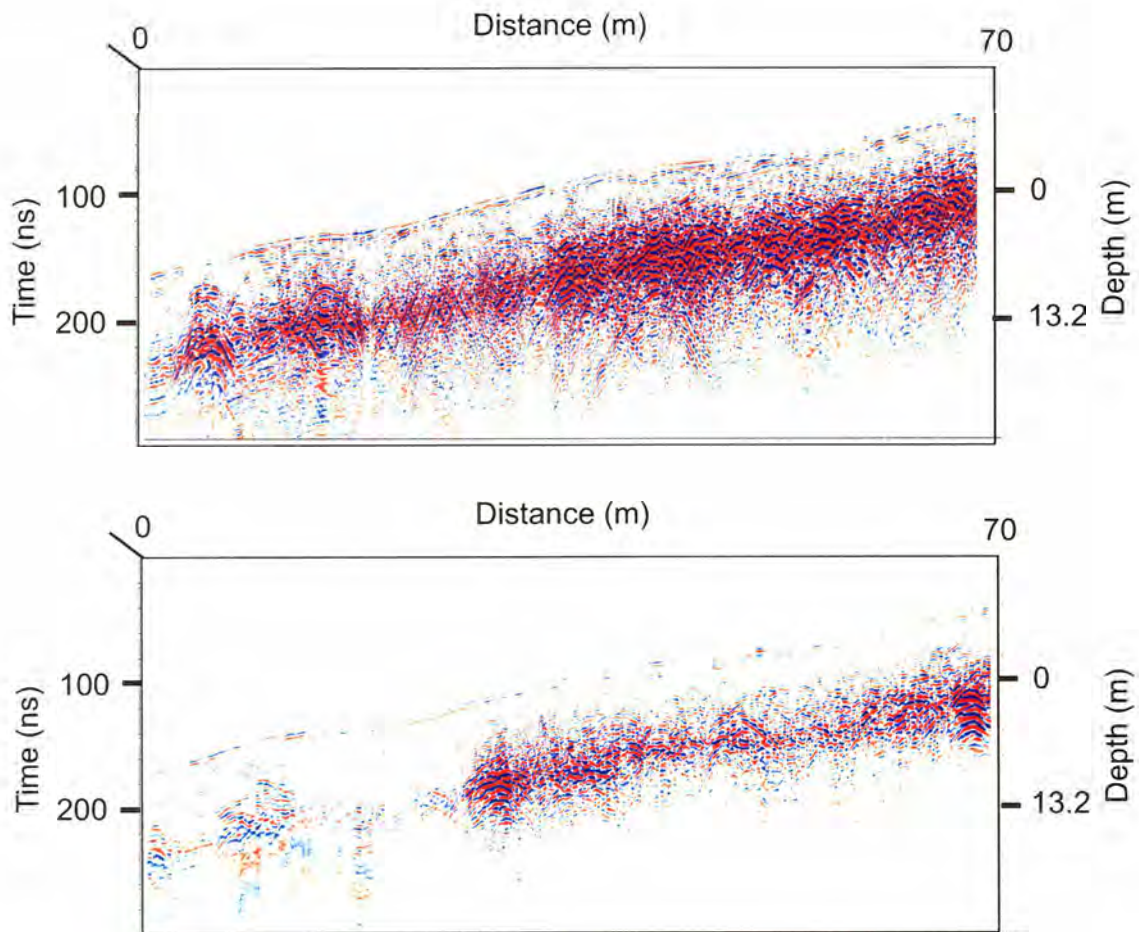


Figure 23. Transect O (top) and transect E (bottom) data corrected for elevation. Overall brightening of winter survey (top).

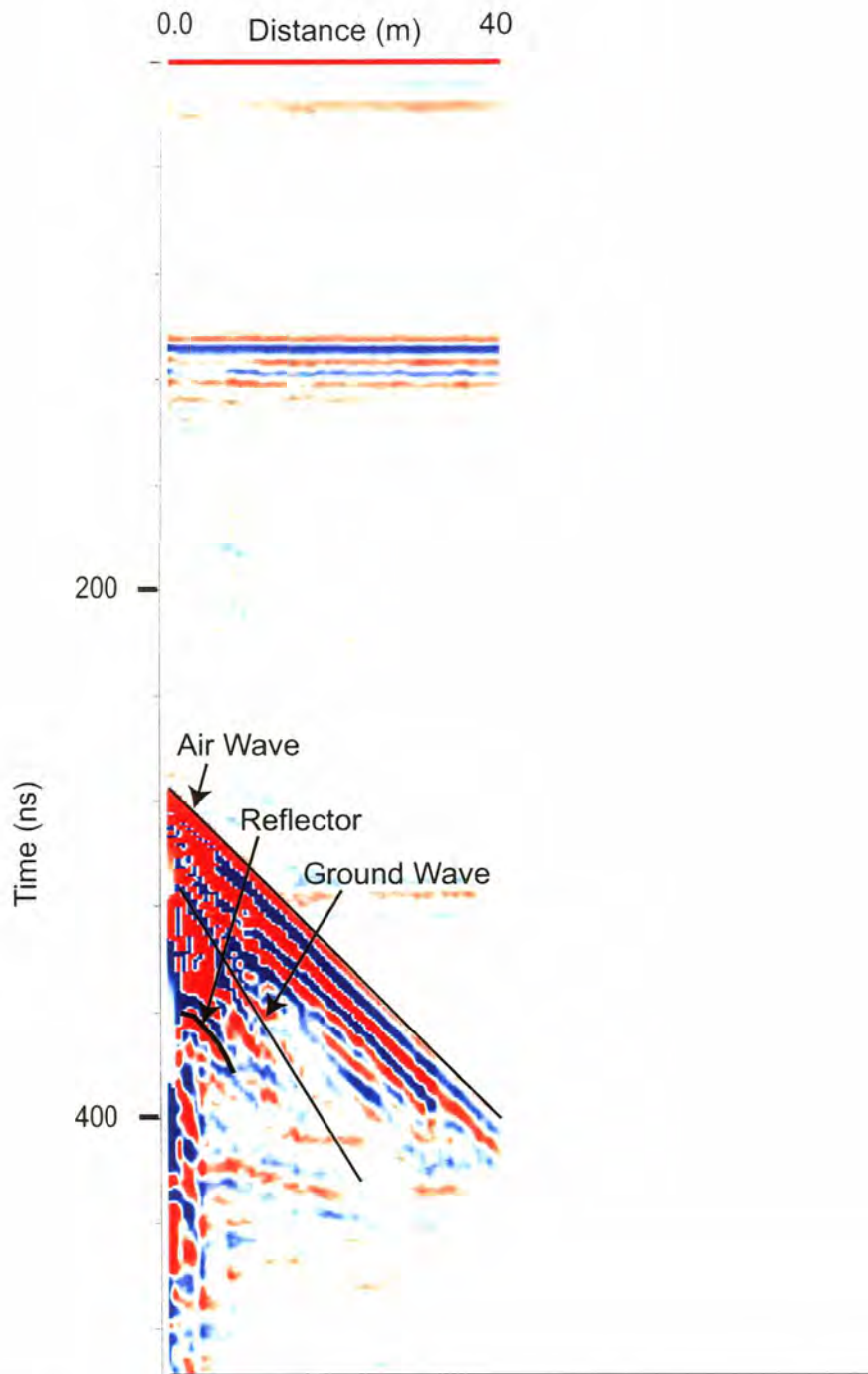


Figure 24. CMP survey results for Tahuya Landslide along Transect I (see Table 2 for distance versus time for reflector).

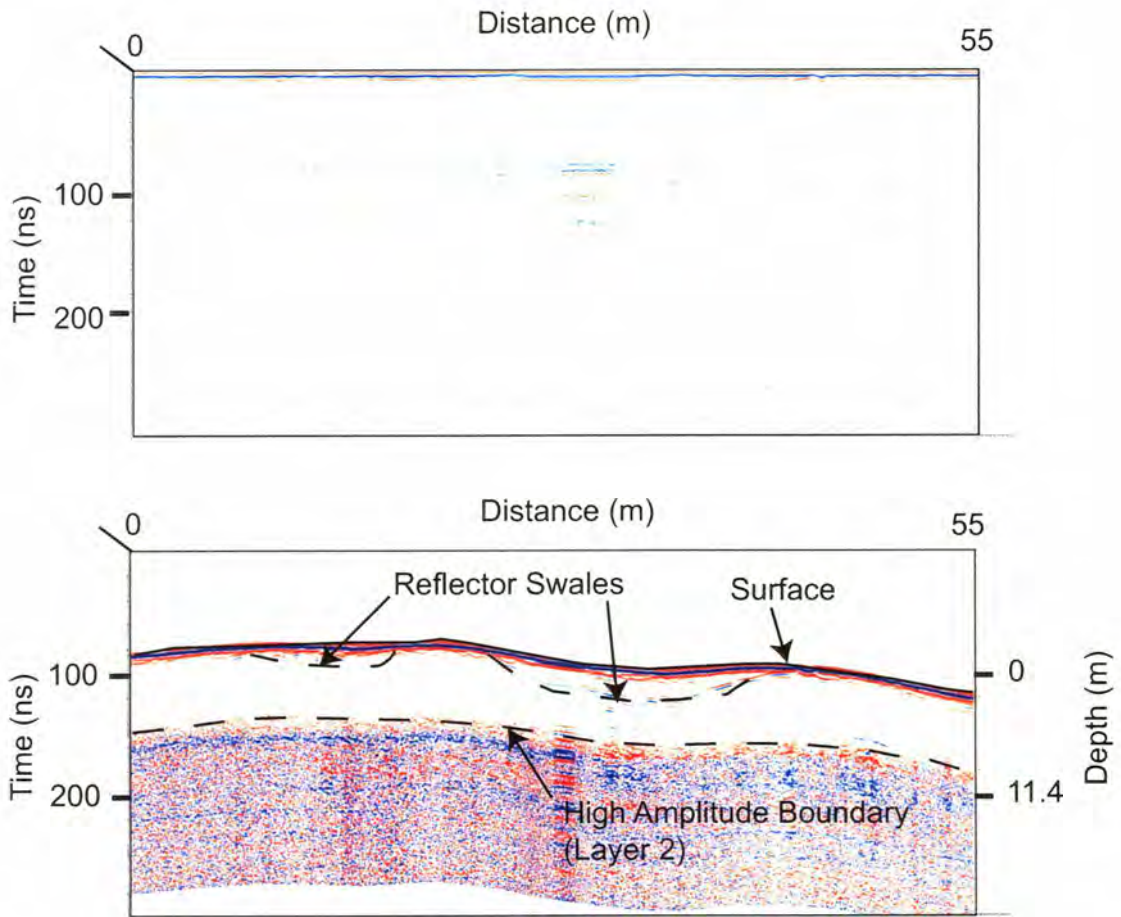


Figure 25. Transect I, Tahuya Landslide; raw (top) and processed (bottom) data corrected for elevation with radar features noted.

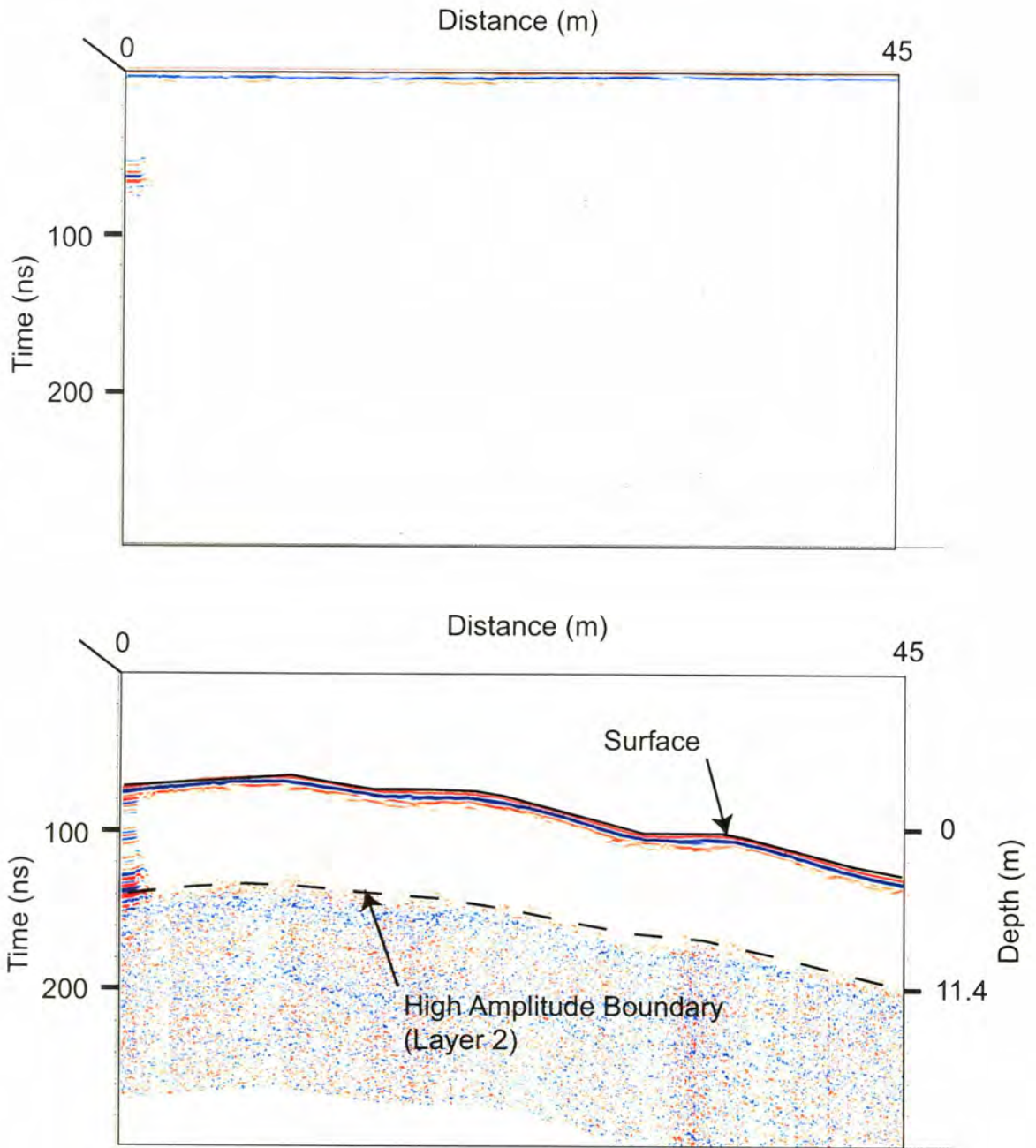


Figure 27. Transect K, Tahuya Landslide; raw (top) and processed (bottom) data corrected for elevation with radar features noted.

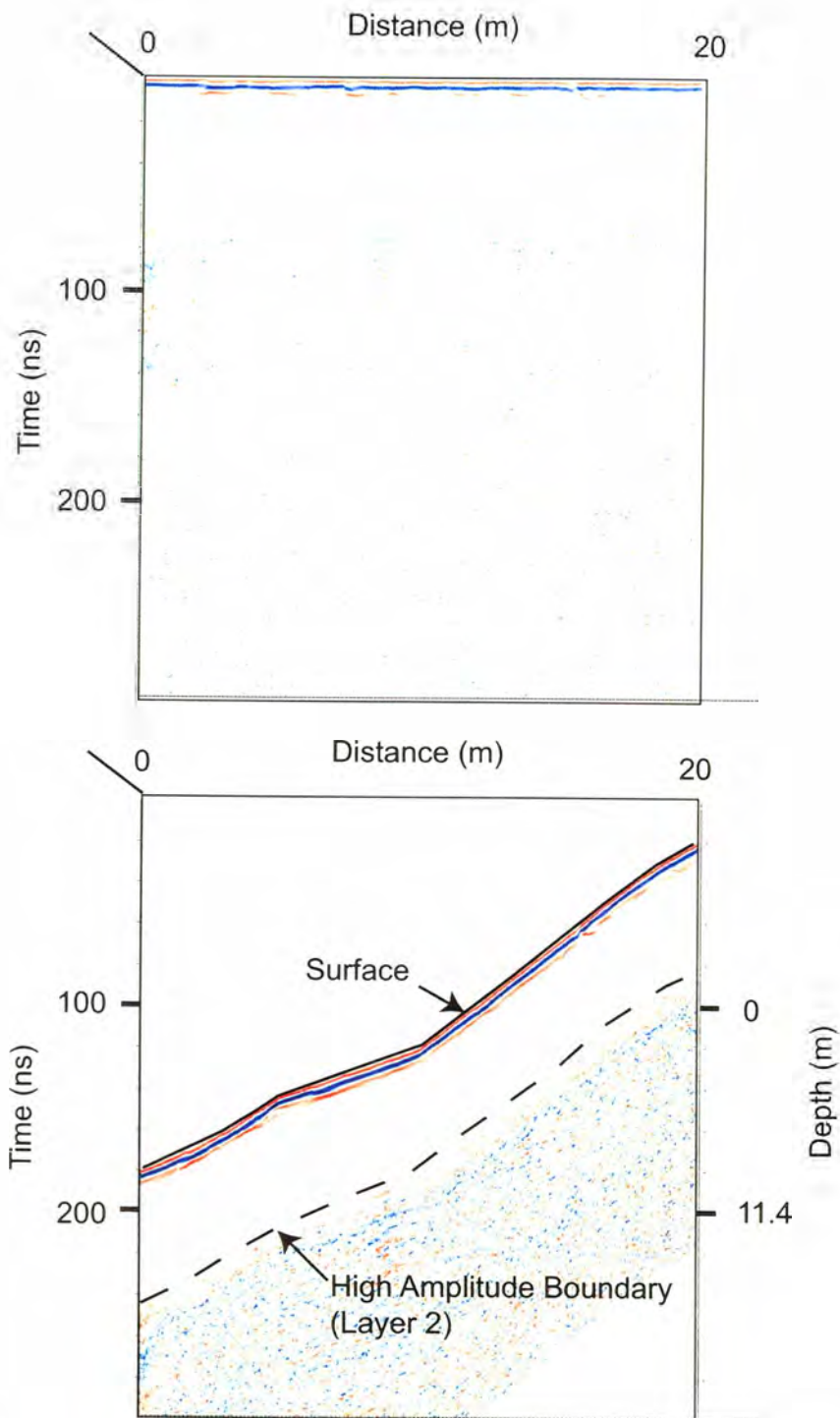


Figure 28. Transect L, Tahuya Landslide; raw (top) and processed (bottom) data corrected for elevation with radar features noted.

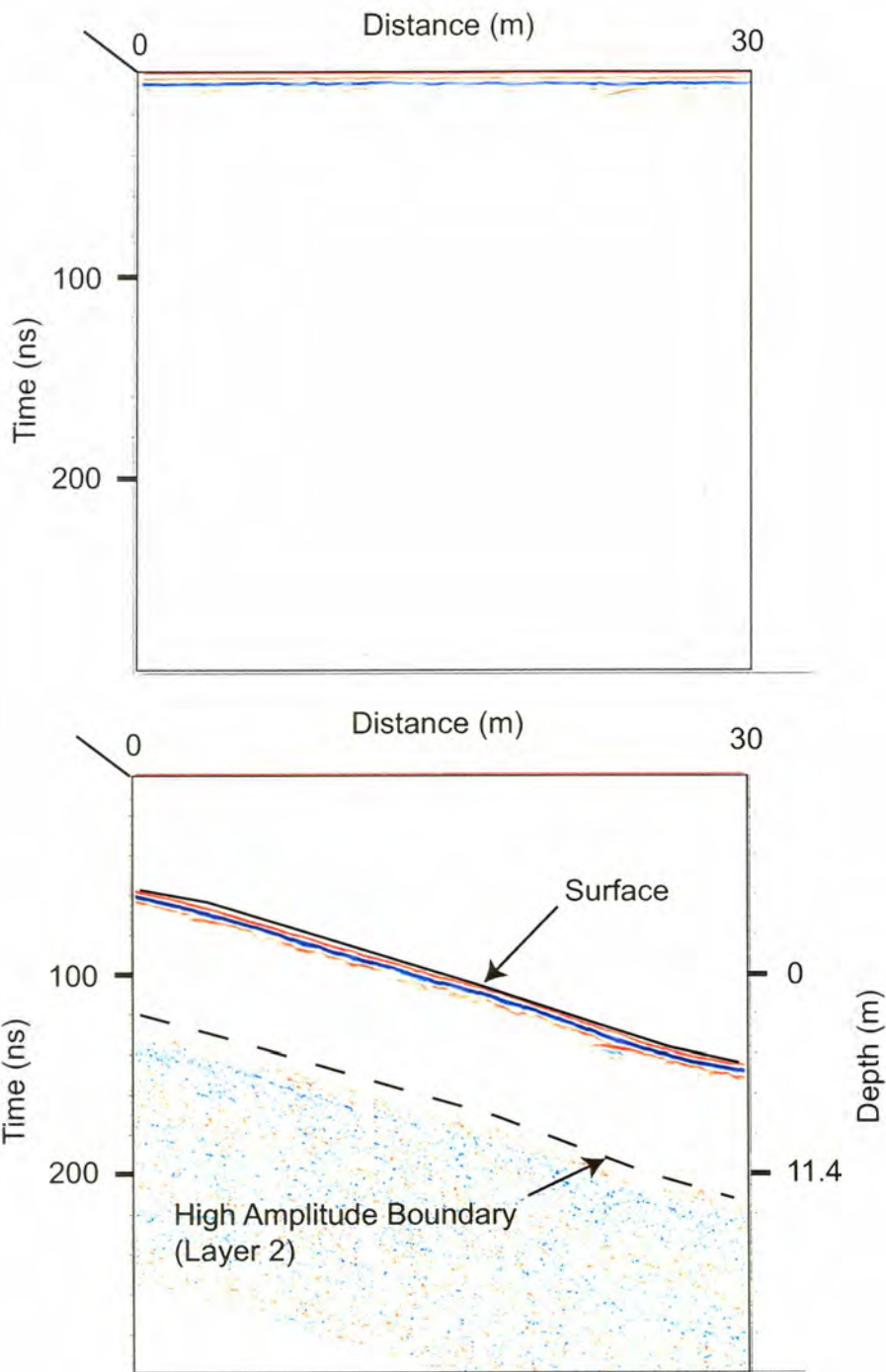


Figure 29. Transect M, Tahuya Landslide; raw (top) and processed (bottom) data corrected for elevation with radar features noted.